

2

# NAVAL POSTGRADUATE SCHOOL

## Monterey, California

AD-A226 061



# THESIS

DTIC  
ELECTE  
AUG 30 1990  
S B D  
Co

A GENERIC SET OF HF ANTENNAS FOR USE  
WITH SPHERICAL MODE  
EXPANSIONS

by

Nedim Katal

March 1990

Thesis Advisor:

Richard W. Adler

Approved for public release; distribution is unlimited

Prepared for:  
USAISEIC  
Ft Huachuca, AZ 85613

183

NAVAL POSTGRADUATE SCHOOL  
MONTEREY, CALIFORNIA 93943

Rear Admiral R.W. West, Jr.


Superintendent

Harrison Shull

Provost

This thesis prepared in conjunction with research sponsored  
by USAISEIC, Ft Huachuca, AZ under MIPR SED-13-89.

Released by:

  
Dean of Faculty and  
Graduate Studies

Unclassified

security classification of this page

## REPORT DOCUMENTATION PAGE

1a Report Security Classification <b>Unclassified</b>			1b Restrictive Markings		
2a Security Classification Authority			3 Distribution Availability of Report		
2b Declassification Downgrading Schedule			Approved for public release; distribution is unlimited.		
4 Performing Organization Report Number(s) NPS 62-90-005			5 Monitoring Organization Report Number(s)		
6a Name of Performing Organization Naval Postgraduate School		6b Office Symbol (if applicable) EC	7a Name of Monitoring Organization Naval Postgraduate School		
6c Address (city, state, and ZIP code) Monterey, CA 93943-5000			7b Address (city, state, and ZIP code) Monterey, CA 93943-5000		
8a Name of Funding Sponsoring Organization USAISEIC		8b Office Symbol (if applicable) ASB-SET-P	9 Procurement Instrument Identification Number		
8c Address (city, state, and ZIP code) Ft. Huachuca, AZ 85613			10 Source of Funding Numbers SED 13-89		
			Program Element No	Project No	Task No
			Work Unit Accession No		
11 Title (include security classification) <b>A GENERIC SET OF HF ANTENNAS FOR USE WITH SPHERICAL MODE EXPANSIONS. (Unclassified)</b>					
12 Personal Author(s) <b>Nedim Katal</b>					
13a Type of Report Master's Thesis		13b Time Covered From To		14 Date of Report (year, month, day) March 1990	
				15 Page Count <b>74</b>	
16 Supplementary Notation The views expressed in this thesis are those of the author and do not reflect the official policy or position of the Department of Defense or the U.S. Government.					
17 Cosan Codes			18 Subject Terms (continue on reverse if necessary and identify by block number)		
Field	Group	Subgroup	Computer Simulation, Numerical Electromagnetics Code (NEC), Tactical HF Field Antennas.		
19 Abstract (continue on reverse if necessary and identify by block number)					
<p>An antenna engineering handbook and database program has been constructed by engineers at the Lawrence Livermore National Laboratory (LLNL) using the Numerical Electromagnetics Code (NEC) antenna modeling program to prepare data performance on tactical field communication antennas used by the Army. It is desirable to have this information installed on a personnel computer (PC), using relational database techniques to select antennas based on performance criteria. This thesis obtains and analyses current distributions and radiation pattern data by using NEC for the following set of four (4) high frequency (HF) tactical generic antennas to be used in future spherical mode expansion work: a quarter wavelength basic whip, a one-wavelength horizontal quad loop, a 564-foot longwire, and a sloping "vee beam" dipole. The results of this study show that the basic whip antenna provides good ground wave communication, but it has poor near vertical incident skywave (NVIS) performance. The current distribution has the characteristics of standing waves. The horizontal quad loop antenna is good for NVIS and medium range skywave communications. The current distribution is sinusoidal and continuous around the loop. The long wire antenna allows short, medium and long range communications and a standing wave current distribution occurs along the antenna axis due to non-termination. The sloping "vee beam" antenna favors long range communication and the current distribution is mainly that of travelling sinusoidal waves. Because of their well-known efficiency, the basic whip and quad loop can be used as reference standards for the spherical mode expansion work. The longwire and sloping "vee beam" antenna are unwieldy, but they are effective as base station antennas.</p>					
20 Distribution Availability of Abstract			21 Abstract Security Classification		
<input checked="" type="checkbox"/> unclassified unlimited <input type="checkbox"/> same as report <input type="checkbox"/> DTIC users			Unclassified		
22a Name of Responsible Individual Richard W. Adler			22b Telephone (include Area code) (408) 646-2352		22c Office Symbol Code EC Ab

DD FORM 1473,84 MAR

83 APR edition may be used until exhausted  
All other editions are obsolete

security classification of this page

Unclassified

Approved for public release; distribution is unlimited.

A Generic Set of HF Antennas for Use with Spherical Mode  
Expansions.

by

Nedim Katal  
First Lieutenant, Turkish Army  
B.S., Turkish Army Academy, 1981

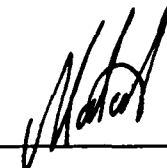
Submitted in partial fulfillment of the  
requirements for the degree of

MASTER OF SCIENCE IN ELECTRICAL ENGINEERING

from the

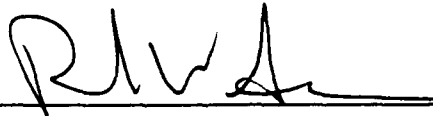
NAVAL POSTGRADUATE SCHOOL  
March 1990

Author:

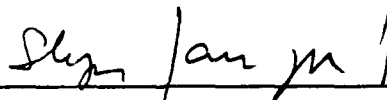


Nedim Katal

Approved by:



Richard W. Adler, Thesis Advisor



Stephen Lauregui, Second Reader



John P. Powers, Chairman,  
Department of Electrical and Computer Engineering

## ABSTRACT

An antenna engineering handbook and database program has been constructed by engineers at the Lawrence Livermore National Laboratory (LLNL) using the Numerical Electromagnetics Code (NEC) antenna modeling program to prepare data performance on tactical field communication antennas used by the Army. It is desirable to have this information installed on a personnel computer (PC), using relational database techniques to select antennas based on performance criteria.

This thesis obtains and analyses current distributions and radiation pattern data by using NEC for the following set of four (4) high frequency (HF) tactical generic antennas to be used in future spherical mode expansion work: a quarter wavelength basic whip, a one-wavelength horizontal quad Loop, a 564-foot longwire, and a sloping "vee beam" dipole.

The results of this study show that the basic whip antenna provides good ground wave communication, but it has poor near vertical incident skywave (NVIS) performance. The current distribution has the characteristics of standing waves. The horizontal quad loop antenna is good for NVIS and medium range skywave communications. The current distribution is sinusoidal and continuous around the loop. The long wire antenna allows short, medium and long range communications and a standing wave current distribution occurs along the antenna axis due to non-termination. The sloping "vee beam" antenna favors long range communication and the current distribution is mainly that of travelling sinusoidal waves.

Because of their well-known efficiency, the basic whip and quad loop can be used as reference standards for the spherical mode expansion work. The longwire and sloping "vee beam" antenna are unwieldy, but they are effective as base station antennas.

iii



Accession For	
NTIS GRA&I	<input checked="checked" type="checkbox"/>
DTIC TAB	<input type="checkbox"/>
Unannounced	<input type="checkbox"/>
Justification	
By	
Distribution/	
Availability Codes	
Dist	Avail and/or Special
A-1	

## THESIS DISCLAIMER

This document was prepared as an account of work sponsored by an agency of the United States Government. Neither the United States Government nor any of their employees, makes any warranty, express or implied, or assumes any legal liability or responsibility for the accuracy, completeness, or usefulness of any information, apparatus, product, or process disclosed, or represents that its use would not infringe privately owned rights. Reference herein to any specific commercial products, process, or service by trade name, trademark, manufacturer, or otherwise, does not necessarily constitute or imply its endorsement, recommendation, or favoring by the United States Government. The views and opinions of authors expressed herein do not necessarily state or reflect those of the United States Government and shall not be used for advertising or product endorsement purposes.

## TABLE OF CONTENTS

I. INTRODUCTION .....	1
A. BACKGROUND .....	1
B. SCOPE OF THE THESIS .....	2
C. SELECTION AND MODELING CRITERIA FOR THE ANTENNAS ...	2
1. Ground and Frequency Selection .....	2
2. Antenna Selection .....	3
D. DESCRIPTION OF THE ANTENNAS .....	4
1. Basic Whip .....	4
2. One Wavelength Horizontal Quad Loop .....	4
3. 564-Foot Longwire .....	4
4. Sloping "Vee Beam" Dipole .....	4
E. INTRODUCTION TO THE NUMERICAL ELECTROMAGNETICS CODE .....	4
II. PERFORMANCE RESULTS OF ANTENNAS .....	10
A. GENERAL .....	10
B. BASIC WHIP WITH 8' GROUND STAKE .....	10
C. ONE WAVELENGTH HORIZONTAL QUAD LOOP .....	11
D. LONG-WIRE ANTENNA .....	24
E. SLOPING VEE BEAM ANTENNA .....	35
III. CONCLUSIONS AND RECOMMENDATIONS .....	45
A. CONCLUSIONS .....	45
B. RECOMMENDATIONS .....	46
APPENDIX A. NEC AND AUXILIARY PROGRAMS .....	47
1. SOMNTX FOR SOMMERFELD / NORTON GROUND METHOD	47
2. THE NUMERICAL GREEN'S FUNCTION (NGF) OPTION .....	47
3. DNPGENEC .....	47
4. PLOT PROGRAMS .....	47
5. RVAL .....	48

6. DIRTLAM .....	48
APPENDIX B. NEC DATA SETS FOR CURRENTS .....	49
APPENDIX C. NUMERICAL METHODS AND TECHNIQUES FOR AN-	
TENNA ANALYSIS .....	53
A. THE METHOD OF SOLUTION .....	53
B. CAPABILITIES OF NEC .....	55
1. Input .....	55
2. Output .....	55
3. Source modeling .....	56
4. Nonradiating Networks and Transmission lines .....	56
5. Loading .....	56
6. Ground Effects .....	56
7. Modeling Guidelines .....	57
C. CONCLUSION .....	58
LIST OF REFERENCES .....	59
INITIAL DISTRIBUTION LIST .....	61



## LIST OF TABLES

Table 1. GROUND TYPES .....	2
-----------------------------	---

## LIST OF FIGURES

Figure 1.	Quarter Wavelength Basic Whip with 8' Ground Stake	5
Figure 2.	One Wavelength Horizontal Quad Loop	6
Figure 3.	564-Foot Longwire	7
Figure 4.	Sloping "Vee Beam" Dipole	8
Figure 5.	Current Distribution of Basic Whip Antenna at 5 MHz.	12
Figure 6.	Elevation Pattern of Basic Whip Antenna at 5 MHz.	13
Figure 7.	Current Distribution of Basic Whip Antenna at 30 MHz.	14
Figure 8.	Elevation Pattern of Basic Whip Antenna at 30 MHz.	15
Figure 9.	Current Distribution of Quad Loop Antenna at 5 MHz.	16
Figure 10.	The YZ-plane pattern of Quad Loop Antenna at 5 MHz.	17
Figure 11.	The XZ-plane pattern of Quad Loop Antenna at 5 MHz.	18
Figure 12.	The XY-plane pattern of Quad Loop Antenna at 5 MHz.	19
Figure 13.	Current Distribution of Quad Loop Antenna at 30 MHz.	20
Figure 14.	The YZ-plane pattern of Quad Loop Antenna at 30 MHz.	21
Figure 15.	The XZ-plane pattern of Quad Loop Antenna at 30 MHz.	22
Figure 16.	The XY-plane pattern of Quad Loop Antenna at 30 MHz.	23
Figure 17.	Current Distribution of Long Wire Antenna at 5 MHz.	26
Figure 18.	Elevation Pattern of Long Wire Antenna at 5 MHz.	27
Figure 19.	Azimuth Pattern of Long Wire Antenna at 5 MHz.	28
Figure 20.	Azimuth Pattern of Long Wire Antenna at 5 MHz.	29
Figure 21.	Azimuth Pattern of Long Wire Antenna at 5 MHz.	30
Figure 22.	Current Distribution of Long Wire Antenna at 30 MHz.	31
Figure 23.	Elevation Pattern of Long Wire Antenna at 30 MHz.	32
Figure 24.	Azimuth Pattern of Long Wire Antenna at 30 MHz.	33
Figure 25.	Azimuth Pattern of Long Wire Antenna at 30 MHz.	34
Figure 26.	Current Distribution of Sloping Vee Antenna at 5 MHz.	37
Figure 27.	Elevation Pattern of Sloping Vee Antenna at 5 MHz.	38
Figure 28.	YZ-Plane Pattern of Sloping Vee Antenna at 5 MHz.	39
Figure 29.	Azimuth Pattern of Sloping Vee Antenna at 5 MHz.	40
Figure 30.	Current Distribution of Sloping Vee Antenna at 30 MHz.	41
Figure 31.	Elevation Pattern of Sloping Vee Antenna at 30 MHz.	42

Figure 32. YZ-Plane Pattern of Sloping Vee Antenna at 30 MHz. . . . .	43
Figure 33. Azimuth Pattern of Sloping Vee Antenna at 30 MHz. . . . .	44

## ACKNOWLEDGEMENTS

The author would like sincerely thank to Profs. Richard W. Adler and James K. Breakall for their patient guidance and knowledge. I also thank my family and my friends for their support.

## I. INTRODUCTION

### A. BACKGROUND

A seven (7) volume antenna engineering handbook has been produced at the Lawrence Livermore National Laboratory (LLNL) using the Numerical Electromagnetics Code (NEC) antenna modeling program for the US Army Information Systems Engineering Center (USAISEC), Ft. Huachuca, Arizona. [Refs. 1,2].

A host of field tactical antenna types and configurations have been characterized for optimizing performance for high frequency (HF) communications when interfaced with existing propagation codes and models.

It is desirable to have all useful antenna information installed in a database program on a personnel computer (PC) for selecting of best candidate antennas for a given operational scenario. Initial work was started on this project several years ago and has continued to date [Ref. 3].

Initial efforts here concentrated on applying existing software and new programs necessary for completing this effort and on producing a computer program for the PC.

Most of the antennas in the antenna handbook are less than a few wavelengths in extent, limiting the directivity. This limitation translates into patterns which are describable in terms of a few low order spherical modes.

A proposal, made by Dr. T. L. Simpson, Electrical and Computer Engineering Department, University of South Carolina, was to solve the problem of pattern generation by finding a more natural and simple way of expressing the currents in terms of a spherical modal expansion. "Since the general solution of the electromagnetic wave equation in spherical coordinates can be conveniently expressed as a sum over a set of orthogonal eigenfunctions, or modes [Refs. 4, 5, 6], one can always express a physically realizable pattern function such as an expansion. In effect, the use of the spatial filtering properties of the antenna reduces the antenna pattern to its fundamentally simplest form." [Ref. 7].

It is desired to investigate and complete the representation of HF antenna patterns using Spherical Mode Expansion. The result of this work will be used to generate patterns on the PC with minimal disk storage requirements and fast execution speed.

## B. SCOPE OF THE THESIS

In order to represent HF antenna patterns using Spherical Mode Expansion, NEC results for radiation pattern calculations and current distribution data are required for the support of research in the spherical modal solutions.

This thesis presents current distribution and radiation pattern data produced by NEC for the HF range of 5 and 30 MHz for the following set of four (4) tactical generic antennas: a quarter wavelength basic whip with 8' ground stake, a one-wavelength horizontal quad loop, a 564-foot longwire, and a sloping "vee beam" dipole.

## C. SELECTION AND MODELING CRITERIA FOR THE ANTENNAS

### 1. Ground and Frequency Selection

Several options are available for modeling antennas which are located near the ground. Either perfect ground or imperfect ground can be specified, with the NEC user supplying values for the conductivity ( $\sigma$ ) and relative permittivity ( $\epsilon_r$ ), in the case of finite ground, as shown by the following table:

Table 1. GROUND TYPES

Conductivity (mhos m)	Relative Permittivity	Land Type
0.00022	2.5	flat desert, cities
0.0012	7.0	mountains; steep rocky hills
0.003	10.0	average ground
0.011	13.0	pastoral land, medium hills
0.065	22.5	rich farm land
0.15	34.0	rice paddy

The ground constants (conductivity and relative permittivity) used throughout this thesis are "average" ground values characteristics of many rural sites, so that the performance calculated by the computer would be similar to the results one could expect to find under typical tactical conditions.

The frequencies selected for this study are 5 MHz, which is the logarithmic mean for frequencies over which near vertical incident skywave (NVIS) communications are conducted, and 30 MHz, which is the highest frequency defined by the International

Radio Consultative Committee (CCIR) for the HF band (3 to 30 MHz). Ionospheric skywave propagation is dominant at these frequencies and is used for skywave links.

The reason for selecting these frequencies is to calculate the performance of the generic antennas at the low and high frequency limits of the HF band. Thus the results bracket the performance over the entire HF band.

## **2. Antenna Selection**

Several criteria were used when selecting the antennas for use in the Antenna Handbook. The following performance criteria were selected as desirable for field conditions:

1. Communication effectiveness.
2. Ruggedness.
3. Easy of construction in the field.
4. Simplicity.

The Antenna Engineering Handbook presently contains the following set of antenna model configurations:

1. Basic whip with and without a radio set.
2. Basic half square.
3. Inverted half square.
4. Folded half square.
5. 3-element half square.
6. Inverted 3-element half square.
7. Horizontal vee beam.
8. Sloping vee beam.
9. Sloping vee beam, legs terminated.
10. Horizontal dipole.
11. Inverted-vee dipole.
12. Horizontal square loop (quad).
13. Vertical triangular loop (delta Loop).
14. Basic longwire.
15. Sloping longwire.
16. Inverted-vee longwire.

From these, a set of four generic antennas mentioned in part B has been selected.

Besides military use, some of the antennas selected for this work are commonly used by amateur, commercial, and maritime HF stations. These were selected because some of them have buried parts, others do not touch the ground, or the physical sizes differ substantially. Some of them are slanted while others have axes parallel to cartesian coordinates, etc. Thus the simulation program can be tested under different conditions for these well-known antennas.

#### **D. DESCRIPTION OF THE ANTENNAS**

##### **1. Basic Whip**

- This antenna is a quarter wavelength long at the operating frequency. It is vertically polarized and is fed against ground.
- The radius of the antenna is 0.015 m.
- It has also an 8' ground stake buried beneath the ground as seen in Figure 1.

##### **2. One Wavelength Horizontal Quad Loop**

- The One wavelength quad loop antenna has one-quarter wavelength sides and is placed horizontally a quarter-wavelength high over the ground plane. The feed point is at one corner.
- It has 0.001 m. radius. The structure is shown in Figure 2.

##### **3. 564-Foot Longwire**

- This is a 564-foot long wire antenna with a 45° slanted feeder, and is placed 40 feet high above the ground. The feeder is driven by a voltage source whose lower end is tied to a 2-foot ground stake.
- The radius of the wire is also 0.001 m. The structure is shown in Figure 3.

##### **4. Sloping "Vee Beam" Dipole**

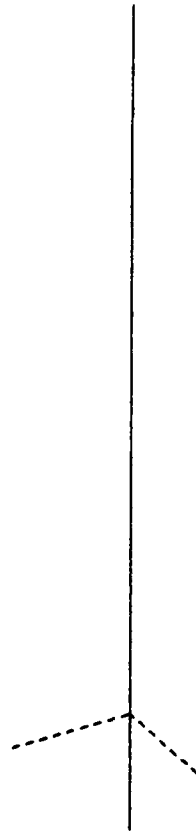
- This antenna may be visualized as two diverging lines terminated through a 600-ohm resistor to a ground stake. It is fed at the apex.
- The apex height is 40 feet above the ground and both ends are 7 feet high. The length of each leg is 528 feet.
- The conductor is also 0.001 m. in radius. The structure is shown in Figure 4.

#### **E. INTRODUCTION TO THE NUMERICAL ELECTROMAGNETICS CODE**

Computer modeling of antennas started in the late 1960's. Since then it has become a powerful tool for antenna design. Computer codes have been developed based on the Method-of-Moments, Geometrical Theory of Diffraction, or integration of Maxwell's



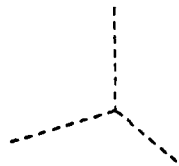
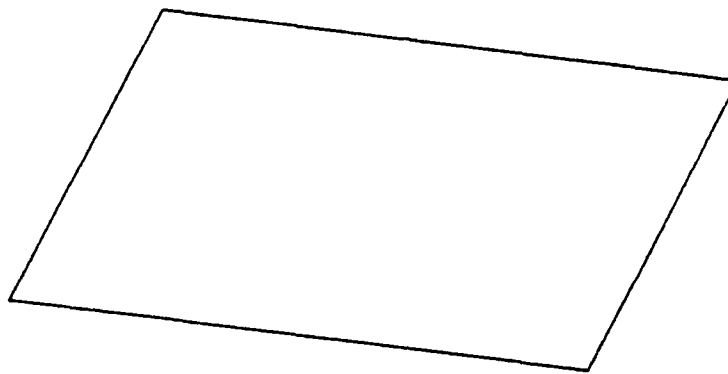
# QUARTER WAVE WHIP



THETA = 60.00 PHI = 60.00 ETA = 90.00

**Figure 1. Quarter Wavelength Basic Whip with 8' Ground Stake**

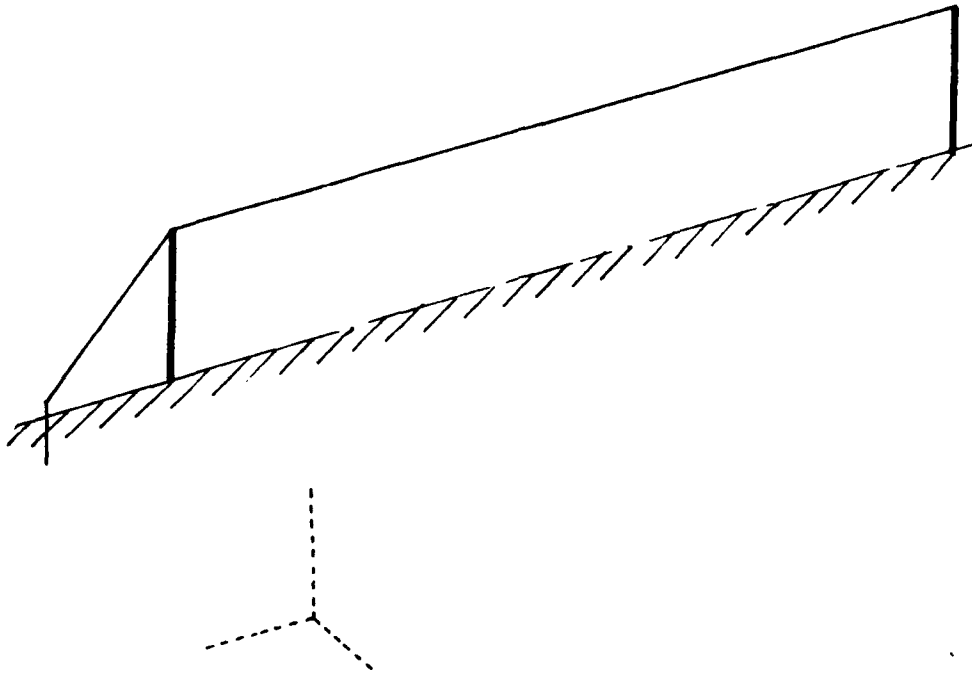
ONE WAVELENGTH HORIZONTAL QUAD LOOP  
QUARTER WAVELENGTH HIGH



THETA = 60.00 PHI = 60.00 ETA = 90.00

Figure 2. One Wavelength Horizontal Quad Loop

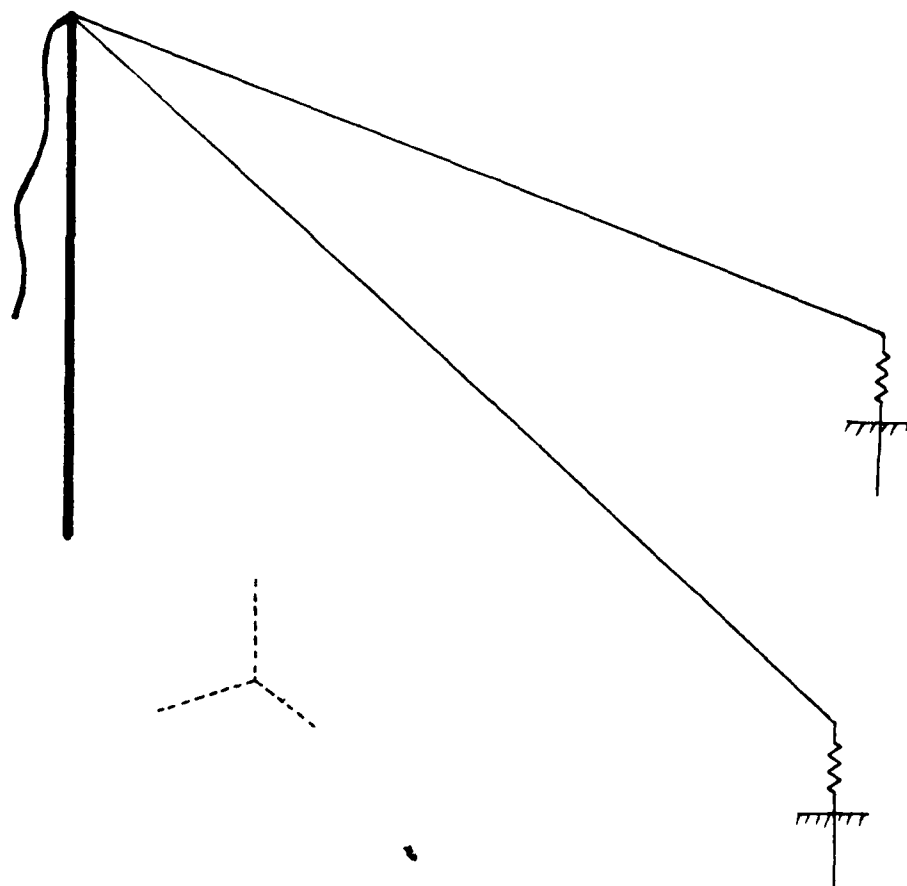
564-FOOT LONGWIRE ANTENNA WITH SLANTED FEEDER



THETA = 60.00 PHI = 60.00 ETA = 90.00

Figure 3. 564-Foot Longwire

# SLOPING "VEE BEAM" DIPOLE



THETA = 60.00 PHI = 60.00 ETA = 90.00

Figure 4. Sloping "Vee Beam" Dipole

Equations. The Numerical Electromagnetics code - Method of Moments [Ref. 2] has become the most widely used of all thin wire codes for modeling resonant-sized antennas. The reasons are that NEC features systematic updating and extension of its capabilities, user-oriented documentation and accessibility of its developers for user assistance.

NEC has been under development for more than ten years (earlier known as BRACT and AMP). It is a hybrid code which uses an Electric Field Integral Equation (EFIE) to model wire like objects and a Magnetic Field Integral Equation (MFIE) to model closed surfaces with time harmonic excitation. NEC is commonly applied to modeling antennas in VLF-to-VHF applications on ships, vehicles or on the ground. A number of features are included for efficient modeling of antennas and scatterers in their environments, including antennas which are interacting with or buried in a finitely conducting ground. Recently, a capability for modeling insulated wires in the air or ground has added to NEC and improved accuracy for electrically small antennas and the treatment of an abrupt change in wire radius [Ref. 8].

The utility of NEC has been enhanced by the development of an interactive graphics utility (IGUANA) [Ref. 9] for developing the model description and examining the results. IGUANA supports both NEC and the Method-of Moments Code MININEC [Ref. 10] for use on personnel computers.

## II. PERFORMANCE RESULTS OF ANTENNAS

### A. GENERAL

- All the antennas have been excited by a voltage source (applied E field source).
- The antennas are driven by 1 kW input power.
- The radiation pattern range is 1 km.
- The wavelengths in the average ground have been calculated and found as 15.6 m for 5 MHz, and 3.1 m for 30 MHz. These data have been used to set segment lengths for buried ground stakes.
- All of the calculations have been done in double precision at 32 bits for accuracy.

### B. BASIC WHIP WITH 8' GROUND STAKE

This antenna is basically a simple monopole with an 8' ground stake. For spot frequency operation, a monopole antenna is satisfactory at a coastal site, but poor at low conductivity sites; its low angle coverage is limited by the amount of ground improvement. Therefore a ground stake has been added to the basic monopole structure.

At 5 MHz, the antenna structure is 15 m above the ground (  $0.25 \lambda$  ), and is modeled by 6 segments, such that all the segment lengths are less than 6 m (  $0.1 \lambda$  ). For the ground stake 3 segments were used due to the smaller wavelength in dirt.

At 30 MHz, the length of the antenna itself is 2.5 m, and it has 5 segments. Also for the buried part, 15 segments were used to model the ground stake.

At 5 MHz, where the ground stake is electrically short, a part of the total base current comes from the return current which flows in the ground beyond the ground stake. The current distribution is shown in Figure 5. It is a standing wave current distribution. The current in the ground stake decreases rapidly and flows outward in the ground. Also the phase is constant which is a characteristic of standing waves.

For this current distribution, a radiation pattern has been calculated and plotted in Figure 6. The maximum field strength occurs at a  $27^\circ$  take-off angle.

The radiation resistance was calculated as

$$R_{rad} = \frac{P_{rad}}{|I^2|} = \frac{500}{|(2.9 + j0.1)^2|} = 58.6 \ \Omega. \quad (1)$$

At 30 MHz the ground stake is about a quarter wavelength long. It provides good ground improvement favoring ground wave communication. The standing wave current distribution is shown in Figure 6. The phase difference between the whip antenna and the ground stake is  $180^\circ$  as expected.

For this frequency, a radiation pattern has been calculated and is shown in Figure 8. The maximum field strength occurs at  $29^\circ$  take-off angle.

The radiation resistance at 30 MHz was found as

$$R_{rad} = \frac{P_{rad}}{|I|^2} = \frac{500}{|(2.9 + j0.1)^2|} = 50.6 \ \Omega. \quad (2)$$

### C. ONE WAVELENGTH HORIZONTAL QUAD LOOP

The one wavelength quad loop antenna can be considered also as a modified folded dipole. By pulling the dipole wires apart at the center, the single-turn quad loop antenna is obtained. The length of each side is  $0.25 \lambda$ .

At 5 MHz, the antenna is placed 15 m above the ground. Each side was modeled by 15 segments. At 30 MHz the antenna is 2.5 m above the ground and each side was modeled by 13 segments.

For a one wavelength perimeter it is reasonable that the current distribution is sinusoidal as shown in Figure 9 for 5 MHz and in Figure 13 for 30 MHz. It is continuous around the loop and the magnitude is minimum at the corners between the feed point sides and the far sides. The phase reverses every  $0.5 \lambda$ .

Principal patterns at 5 MHz are shown in the following order; Figure 10 shows the YZ-plane pattern plot of  $E_\theta$ . In this plane the half-power beamwidth (HPBW) is  $76^\circ$ ; Figure 11 shows the XZ-plane pattern plot of  $E_\theta$  and the HPBW is  $118^\circ$ ; Figure 12 shows the XY-plane pattern plot of  $E_\phi$ .

The radiation resistance was calculated as

$$R_{rad} = \frac{1000}{|(1.9 + j1.7)(-1.9 - j1.7)|} = 142.9 \ \Omega. \quad (3)$$

At 30 MHz the YZ-plane pattern plot of  $E_\theta$  is shown in Figure 14 with HPBW =  $74^\circ$ ; Figure 15 shows the XZ-plane pattern plot of  $E_\theta$  with HPBW =  $116^\circ$ ; Figure 16 shows the XY-plane pattern plot of  $E_\phi$ . The radiation resistance is

$$R_{rad} = \frac{1000}{|(1.9 + j1.9)(-1.9 - j1.9)|} = 132.3 \ \Omega. \quad (4)$$

QUARTER WAVE WHIP OVER AVE. GROUND / 5 MHz  
WITH 8" GROUND STAKE/INCLUDING THE GND STAKE CURRENT

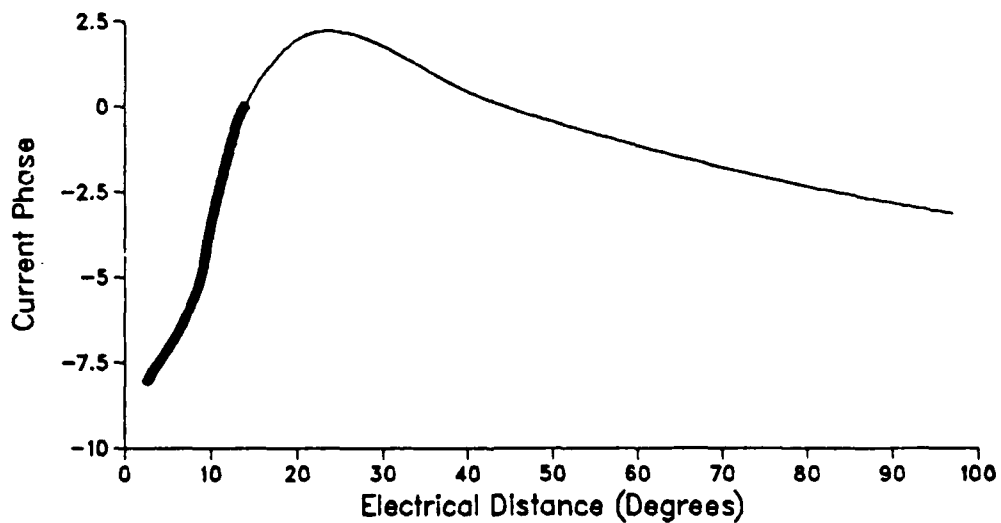
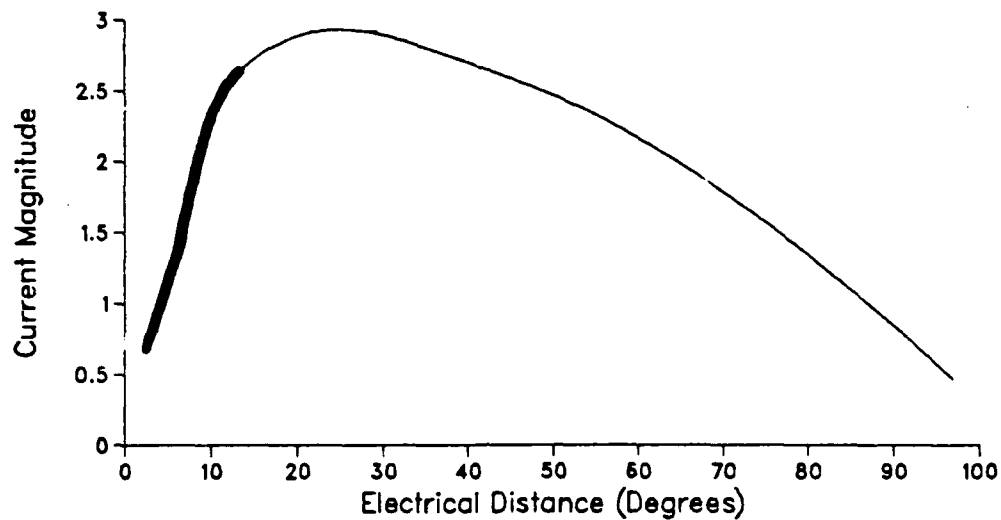


Figure 5. Current Distribution of Basic Whip Antenna at 5 MHz.: Bold line indicates the current distribution on the ground stake.



QUARTER WAVE WHIP WITH 8' GROUND STAKE OVER AVERAGE GND.  
ELEVATION PATTERN / FREQ=5 MHZ.

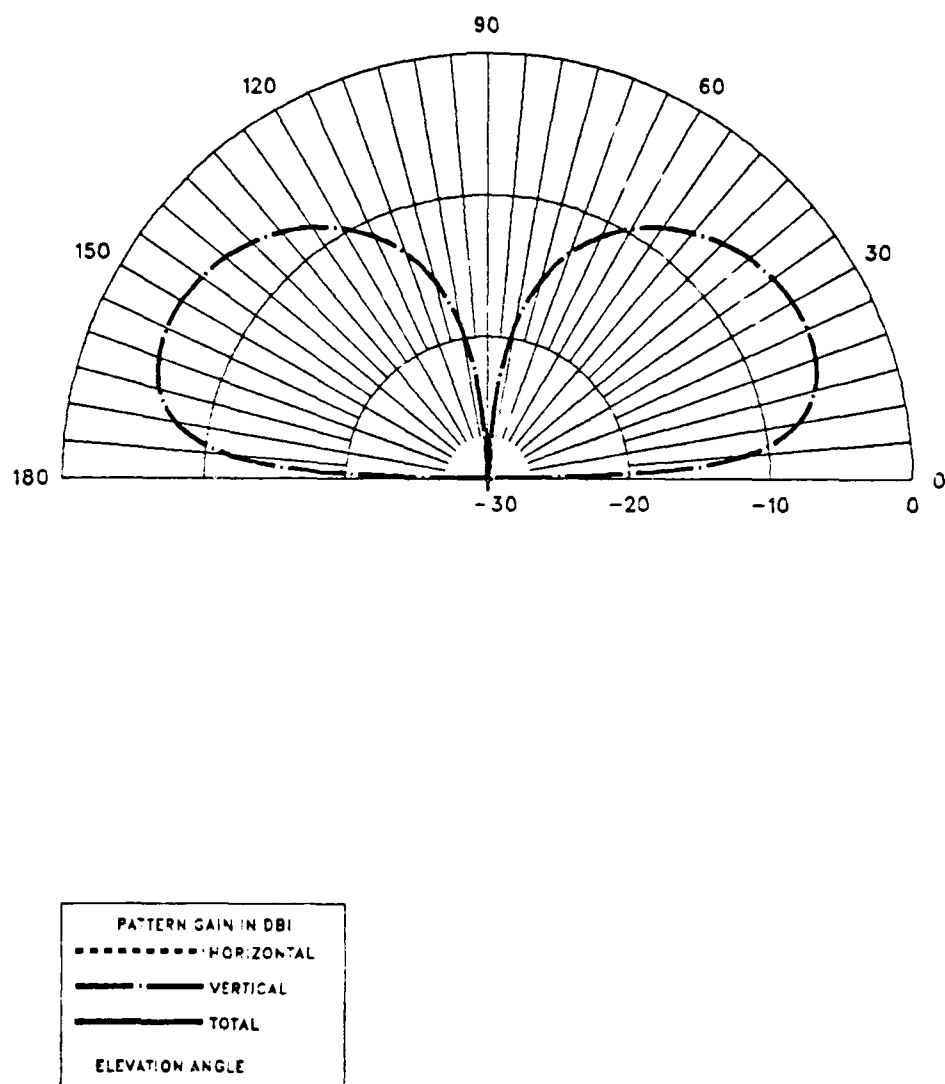


Figure 6. Elevation Pattern of Basic Whip Antenna at 5 MHz:  
 $\epsilon_r = 10.0, \sigma = 0.003$

QUARTER WAVE WHIP WITH 8' GROUND STAKE / FREQ= 30 MHZ.  
OVER AVERAGE GROUND / INCLUDING THE GND. STAKE CURRENT

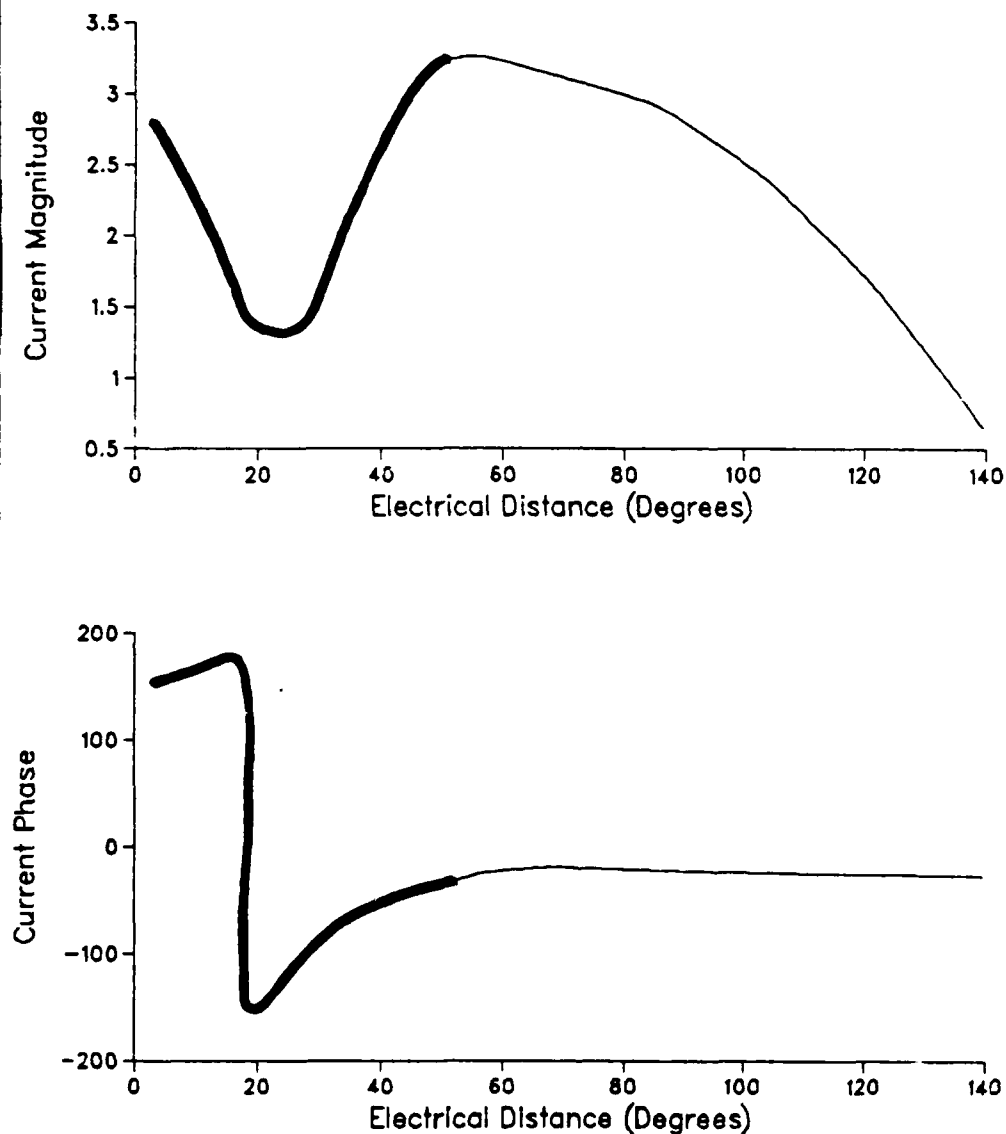


Figure 7. Current Distribution of Basic Whip Antenna at 30 MHz.: Bold line indicates the current distribution on the ground stake.

QUARTER WAVE WHIP WITH 8' GROUND STAKE OVER AVERAGE GROUND.  
ELEVATION PATTERN / FREQ=30 MHZ.

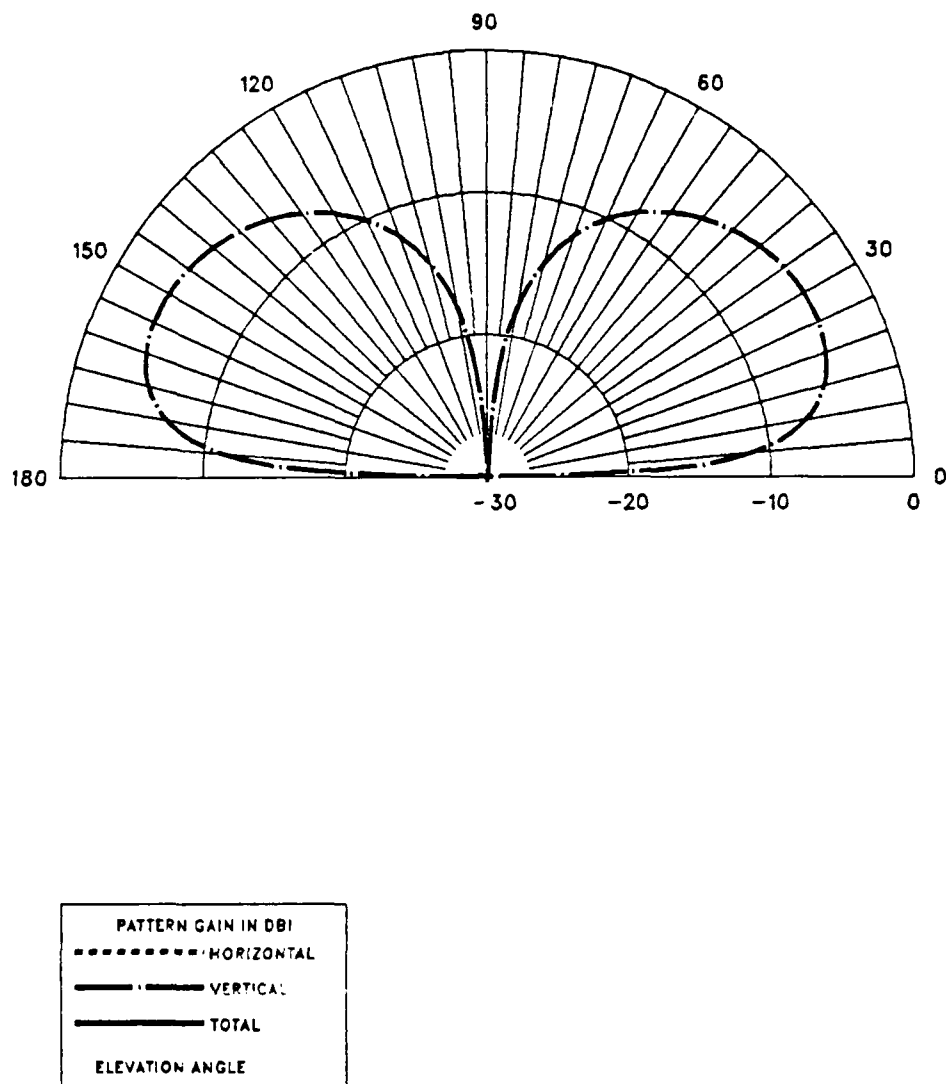


Figure 8. Elevation Pattern of Basic Whip Antenna at 30 MHz.:  
 $\epsilon_r = 10.0, \sigma = 0.003$

ONE WAVELENGTH HORIZONTAL QUAD LOOP / FREQ= 5 MHZ.  
OVER AVERAGE GROUND / HEIGHT= 0.25 WAVELENGTH.

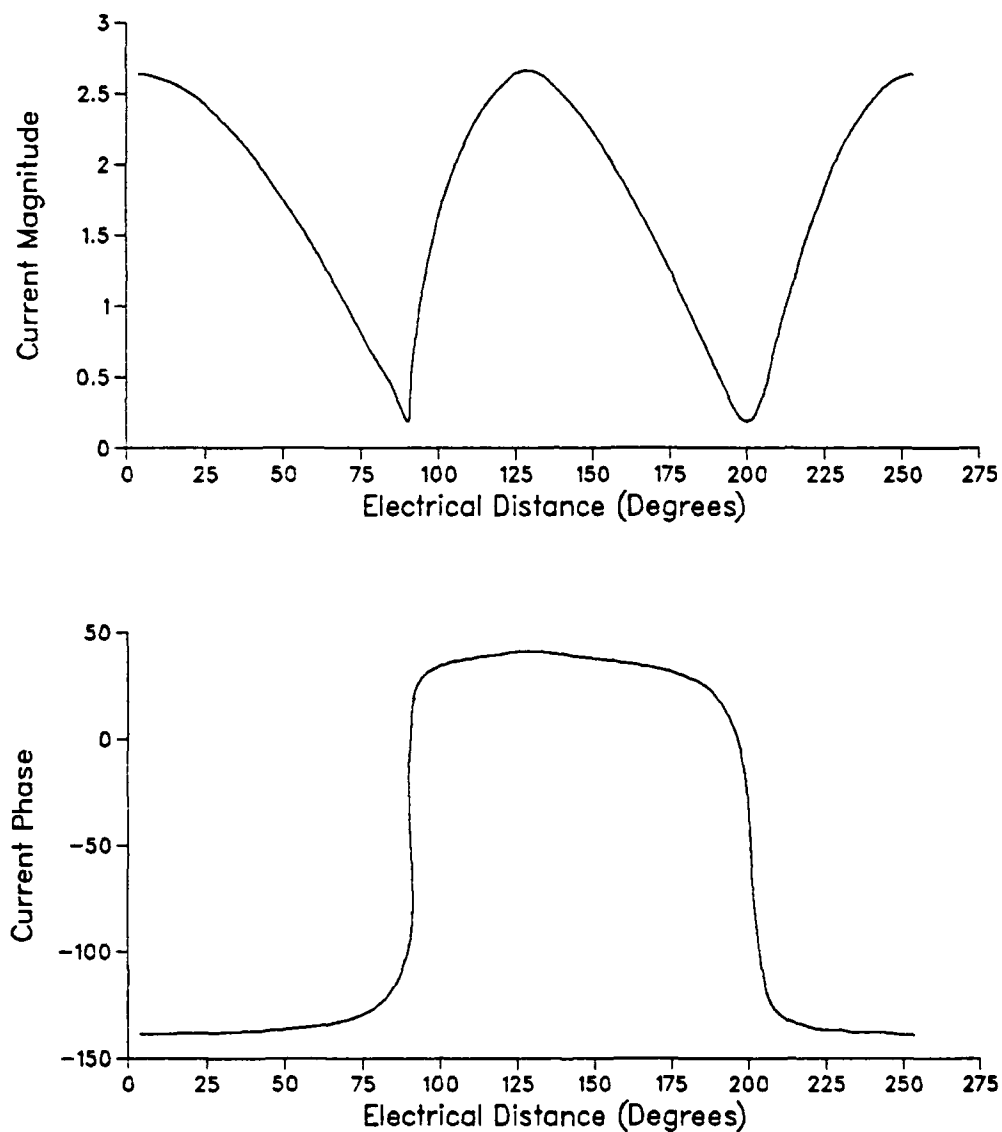


Figure 9. Current Distribution of Quad Loop Antenna at 5 MHz.

ONE WAVELENGTH HORIZONTAL QUAD LOOP / HEIGHT=.25 WAVELENGTH  
OVER AVERAGE GROUND / ELEVATION PATTERN PHI=90 / FREQ=5 MHZ.

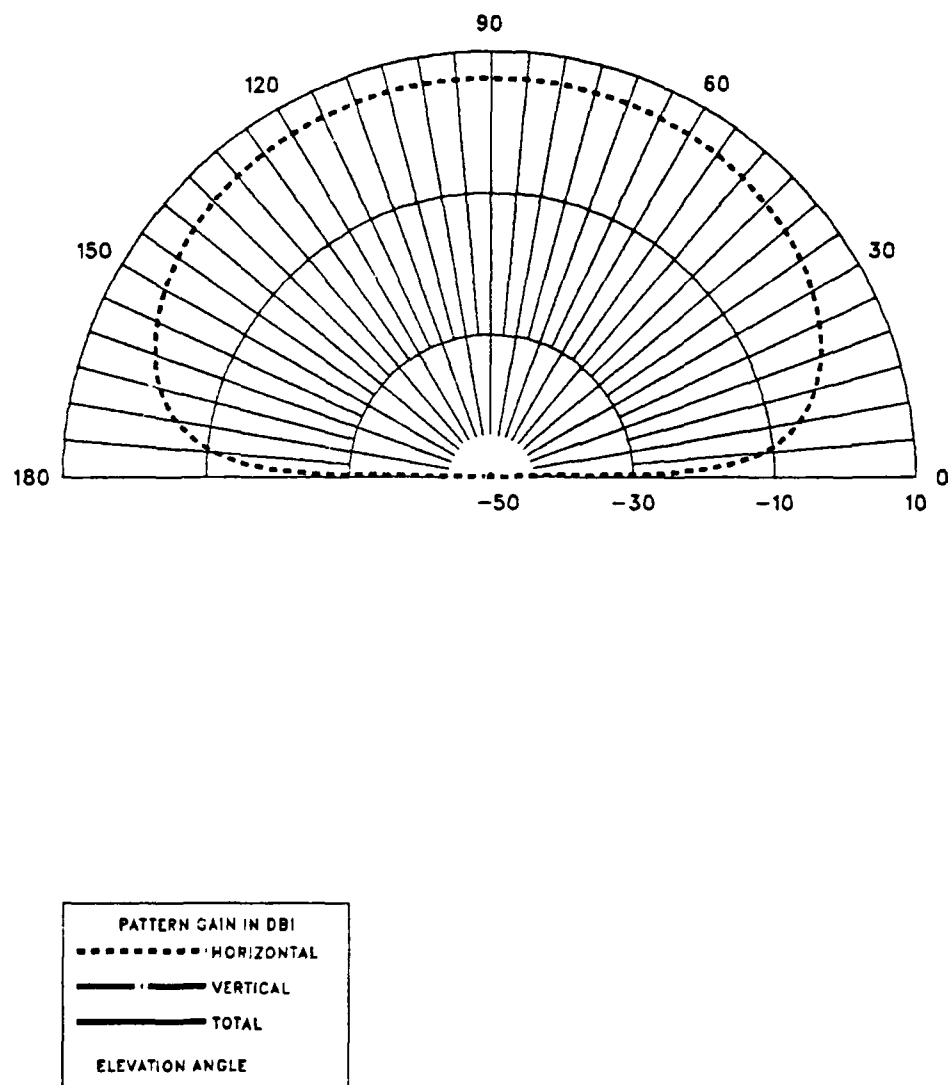


Figure 10. The YZ-plane pattern of Quad Loop Antenna at 5 MHz.:  
 $\epsilon_r = 10.0, \sigma = 0.003$

ONE WAVELENGTH HORIZONTAL QUAD LOOP / HEIGHT=.25 WAVELENGTH  
OVER AVERAGE GROUND / ELEVATION PATTERN PHI=0 / FREQ=5 MHZ.

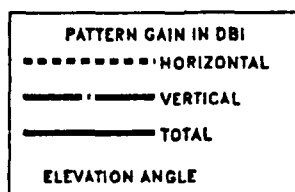
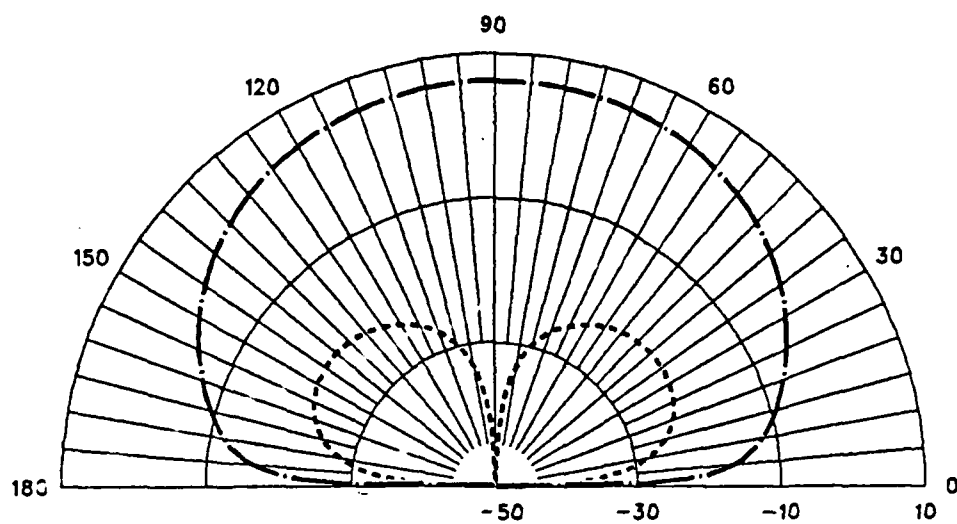


Figure 11. The XZ-plane pattern of Quad Loop Antenna at 5 MHz.:  
 $\epsilon_r = 10.0, \sigma = 0.003$

ONE WAVELENGTH HORIZONTAL QUAD LOOP / HEIGHT=.25 WAVELENGTH  
OVER AVERAGE GROUND / AZIMUTH PATTERN / FREQ=5 MHZ.

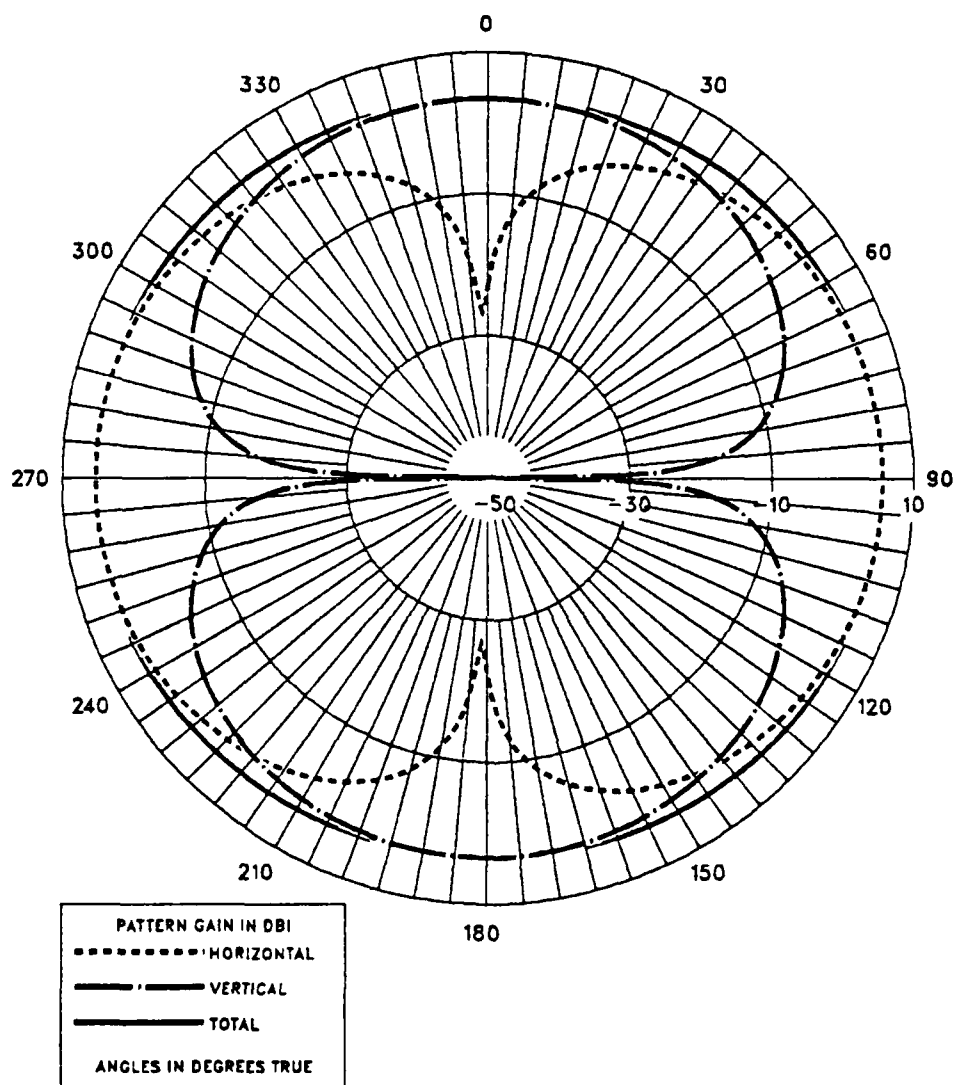


Figure 12. The XY-plane pattern of Quad Loop Antenna at 5 MHz.:  
 $\epsilon_r = 10.0, \sigma = 0.003$

ONE WAVELENGTH HORIZONTAL QUAD LOOP / FREQ= 30 MHZ.  
OVER AVERAGE GROUND / HEIGHT= 0.25 WAVELENGTH.

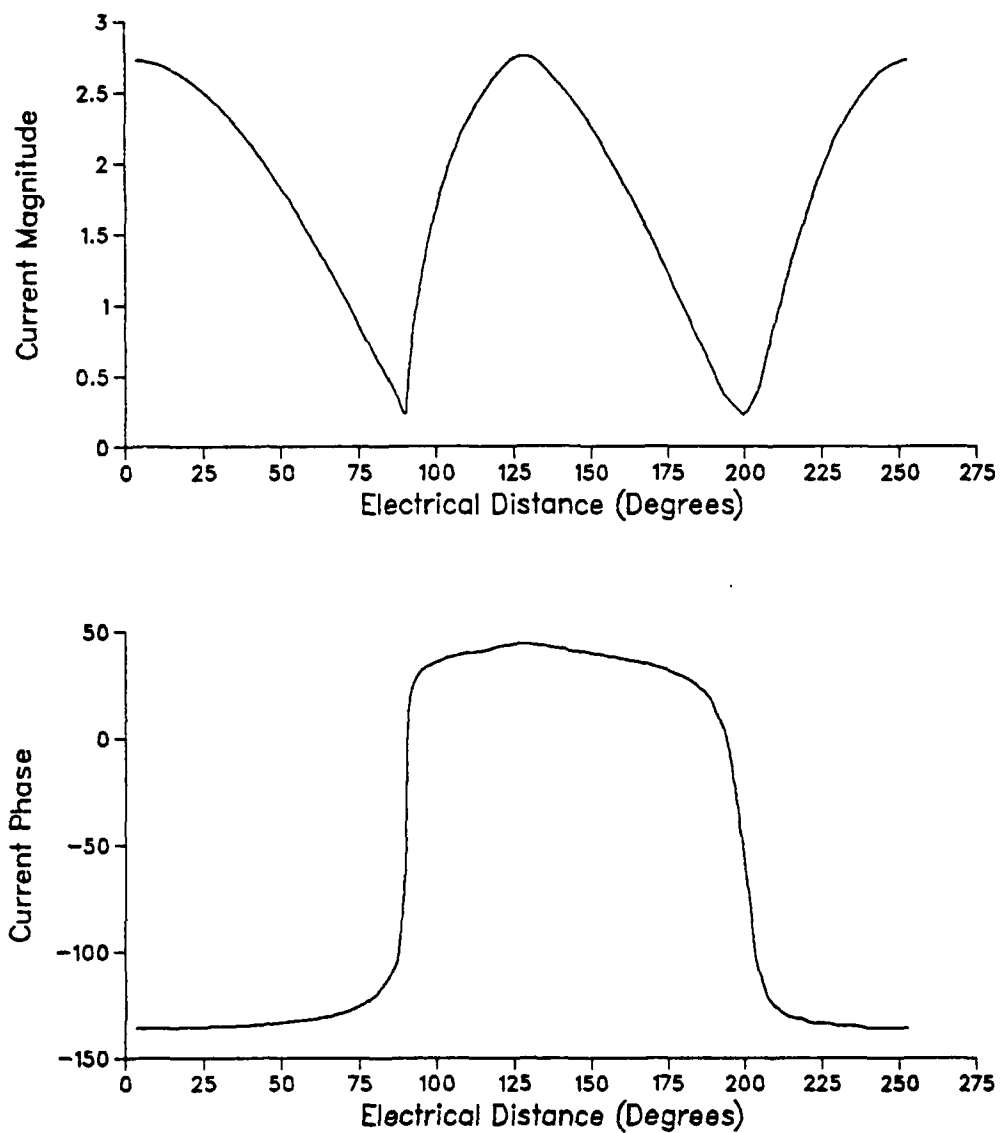


Figure 13. Current Distribution of Quad Loop Antenna at 30 MHz.



ONE WAVELENGTH HORIZONTAL QUAD LOOP / HEIGHT=.25 WAVELENGTH  
OVER AVERAGE GROUND / ELEVATION PATTERN PHI=90 / FREQ=30 MHZ

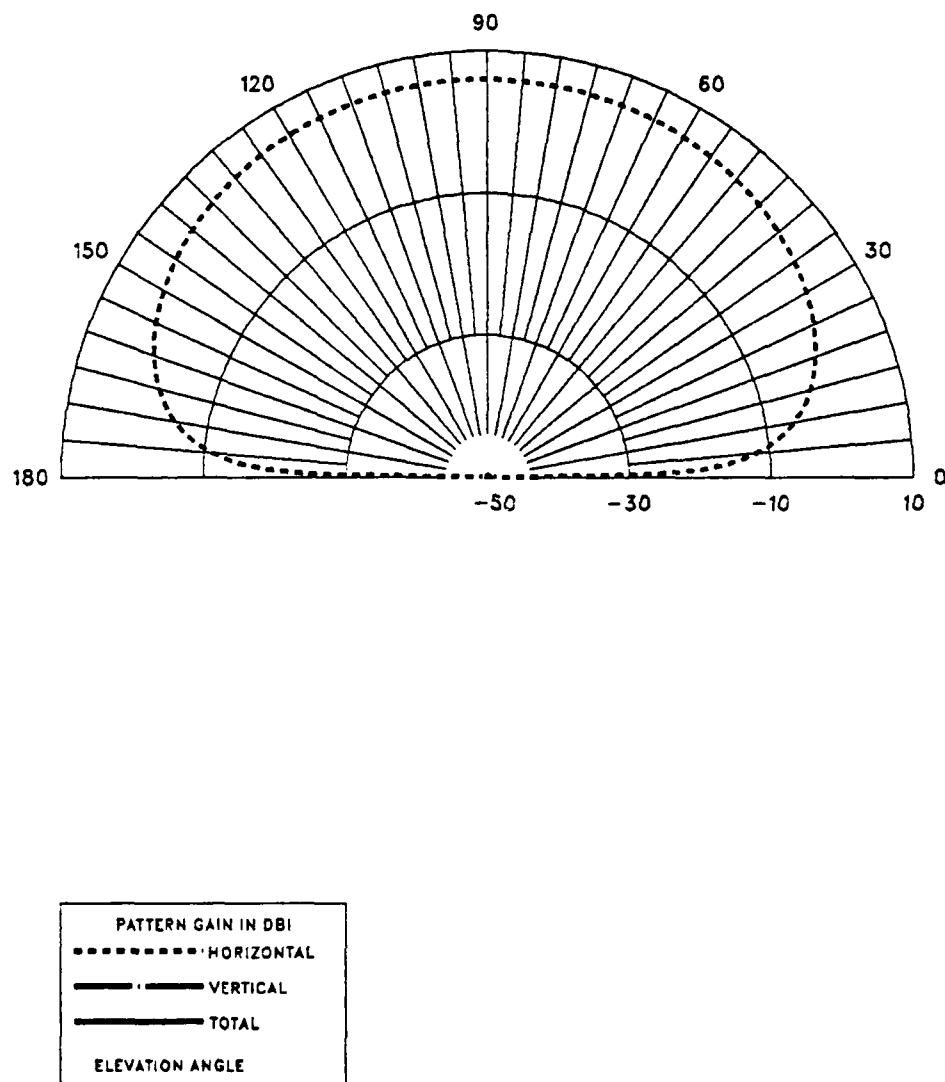


Figure 14. The YZ-plane pattern of Quad Loop Antenna at 30 MHz:  
 $\epsilon_r = 10.0, \sigma = 0.003$

ONE WAVELENGTH HORIZONTAL QUAD LOOP / HEIGHT=.25 WAVELENGTH  
OVER AVERAGE GROUND / ELEVATION PATTERN PHI=0 / FREQ=30 MHZ.

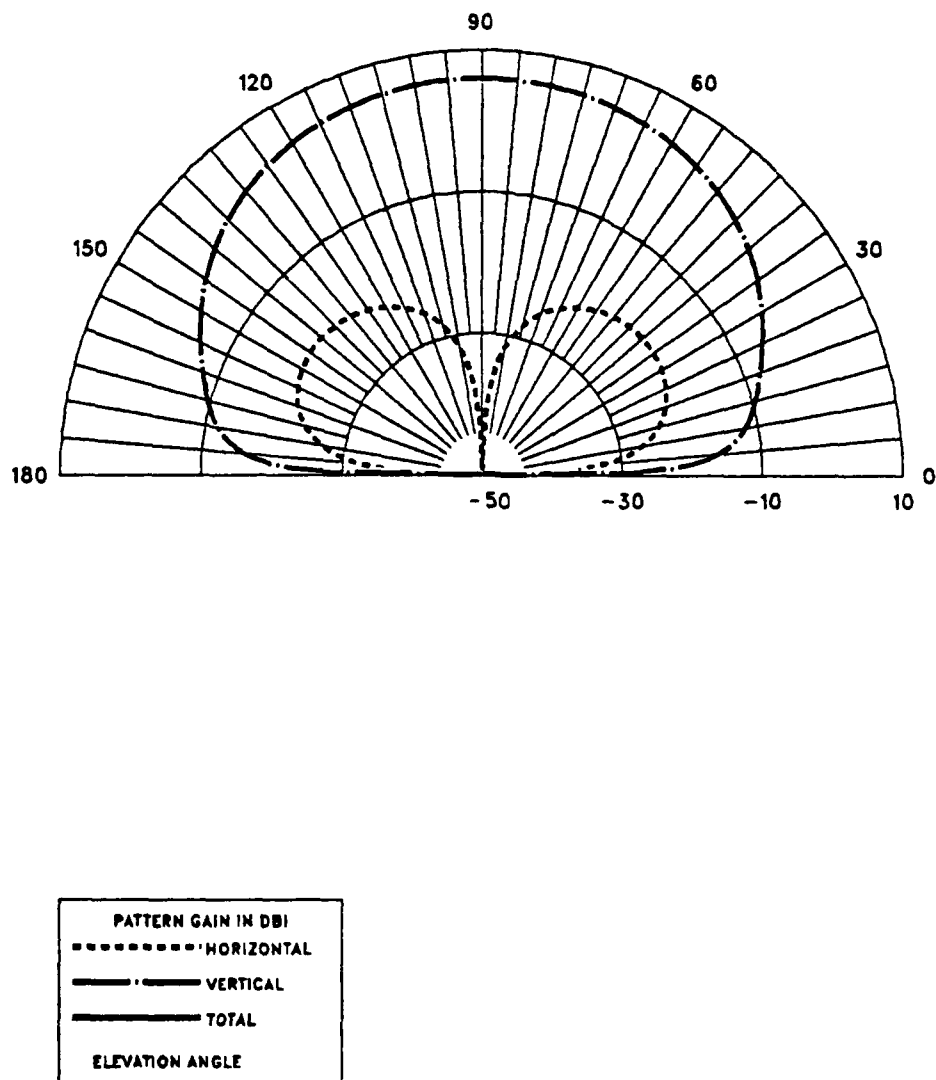


Figure 15. The XZ-plane pattern of Quad Loop Antenna at 30 MHz:  
 $\epsilon_r = 10.0, \sigma = 0.003$

ONE WAVELENGTH HORIZONTAL QUAD LOOP / HEIGHT=.25 WAVELENGTH  
OVER AVERAGE GROUND / AZIMUTH PATTERN / FREQ=30 MHZ.

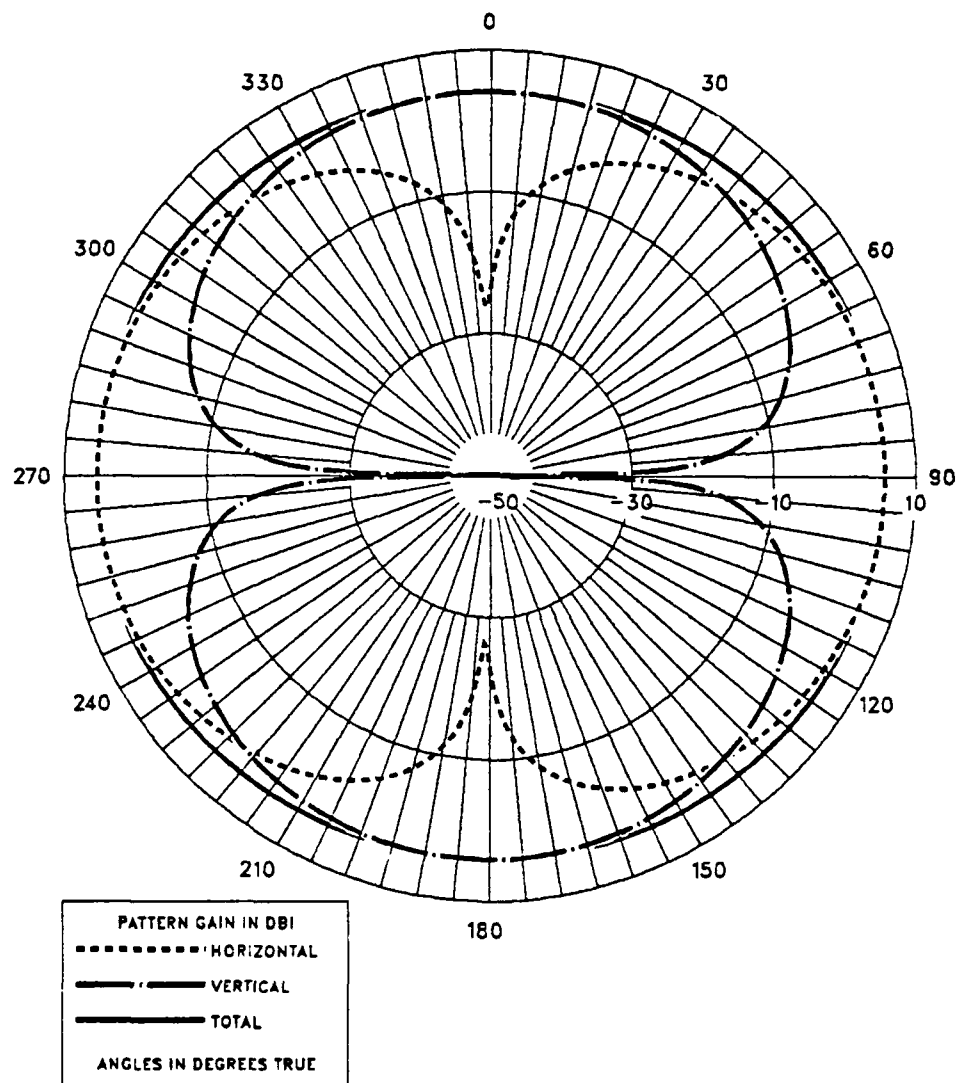


Figure 16. The XY-plane pattern of Quad Loop Antenna at 30 MHz.:  
 $\epsilon_r = 10.0, \sigma = 0.003$

#### D. LONG-WIRE ANTENNA

The wire antennas introduced so far have been resonant-size antennas. The wave travelling outward and reflected from the end sets up a standing-wave type of current distribution. From this section on, non-resonant size antennas will be introduced.

A long-wire antenna is one that is greater than one halfwave length long. When such antennas are unterminated at the end, the current distribution is mainly that of a standing wave. If the antenna is cut to a resonant length, the input impedance will be resistive. The theoretical current distribution is a sinusoidal standing wave. But because of the loss due to radiation, the actual radiation pattern differs from the theoretical calculation. The first recognizable difference is that the lobes tilt toward the unfed end. This difference between actual patterns and theoretical patterns (based on standing waves only) is much less in the case of center-fed antennas.

If a longwire is terminated in a resistance equal to its characteristic impedance, the current distribution is mainly that of a travelling wave. The longer the wire, the smaller will be the angle between the wire and the main lobe. The important difference between the patterns of terminated and unterminated wire antennas is the absence of large rear lobes in the terminated case.

In this study the long wire was 564 feet long and placed 40 feet above the ground. It was unterminated.

At 5 MHz the longwire is on the order of 3 wavelengths (171.9 m) and was modeled by 51 segments. Also this antenna has a 45° slanted feeder segmented by 8 pieces. This feeder was driven by a voltage source whose lower end is tied to a 2-foot ground stake. This ground stake was radius tapered and had 2 segments. At 30 MHz the antenna is approximately 17 wavelengths long and has 200 segments. The slanted feeder was modeled by 45 segments and the ground stake had 4 segments.

For the unterminated case with a pure sinusoidal current distribution (standing wave), the source current can be expressed as a superposition of two uniform waves travelling in opposite directions as

$$I(x) = I_0 \sin[m\pi(\frac{x}{L} + 0.5)] \quad (5)$$

where  $m$  is an integer equal to  $\frac{Lk}{\pi}$ ;  $L$  is the length of the antenna, and  $k$  is the wavenumber ( $\frac{2\pi}{\lambda}$ ).

Figure 17 shows the current distribution at 5 MHz. Standing waves occur along the antenna axis due to non-termination. Also the magnitude decreases slightly due to radiation. The phase also reverses every half wavelength.

Figure 18 shows the elevation pattern at 5 MHz. It is symmetrical about the Z-axis and has a main beam calculated by

$$\alpha_m = \cos^{-1} \left( 1 - \frac{0.371}{L/\lambda} \right) \quad (6)$$

which is  $30^\circ$ , and additional beams in every  $\alpha = 180 - \alpha_m$  direction providing good NVIS, medium range, and long range communications.

Figure 19 shows the azimuth pattern for a  $30^\circ$  take-off angle. Figure 20 shows the same pattern for a  $60^\circ$  take-off angle. Figure 21 shows the azimuth pattern for an  $80^\circ$  take-off angle. All the radiation patterns above are symmetric along the antenna axes and the vertical gains are dominant to the horizontal gains.

Radiation resistance at this frequency was calculated as

$$R_{rad} = \frac{500}{|(0.8 + j1.1)^2|} = 247.4 \ \Omega. \quad (7)$$

Figure 22 shows the current distribution at 30 MHz. Standing waves exist as in the former case but the effect of losses is higher than for the same antenna at 5 MHz. In addition, there are also a few travelling waves. The minimum magnitude of the current occurs in the middle of the antenna.

Figure 23 shows the elevation pattern at 30 MHz. It has a main beam at  $13^\circ$ . Although the radiation pattern has symmetry about the z-axis, the gain of the front lobe is larger than the back lobe.

Figure 24 and 25 show the azimuth patterns for  $15^\circ$  and  $25^\circ$  take-off angles respectively. Both radiation patterns show the main lobe in the forward direction larger than in the reverse direction. This indicates also the existence of travelling waves on the antenna.

Radiation resistance at this frequency was calculated as

$$R_{rad} = \frac{500}{|(1.1 - j1.2)^2|} = 171.1 \ \Omega. \quad (8)$$

564-FOOT LONGWIRE WITH SLANTED FEEDER / FREQ= 5 MHZ.  
OVER AVERAGE GROUND / HEIGHT = 40 FEET.

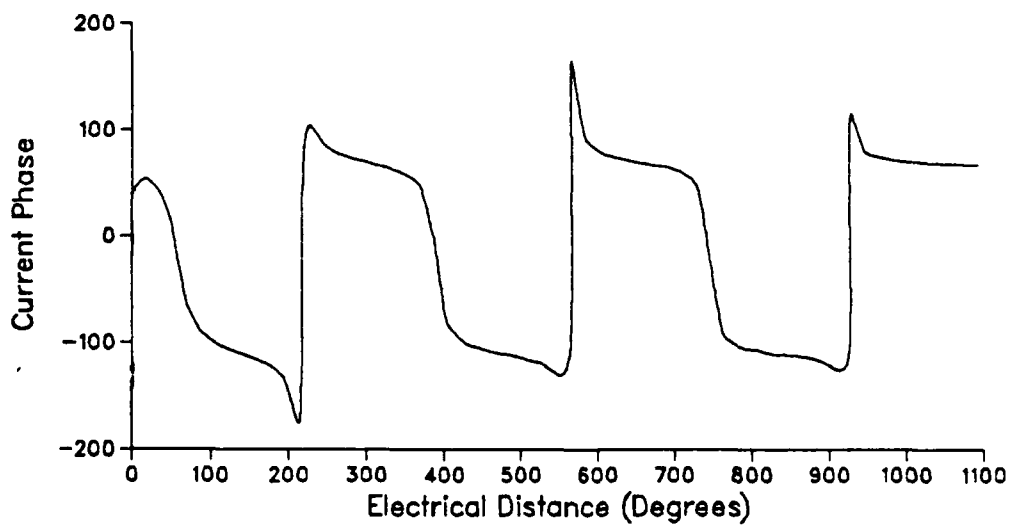
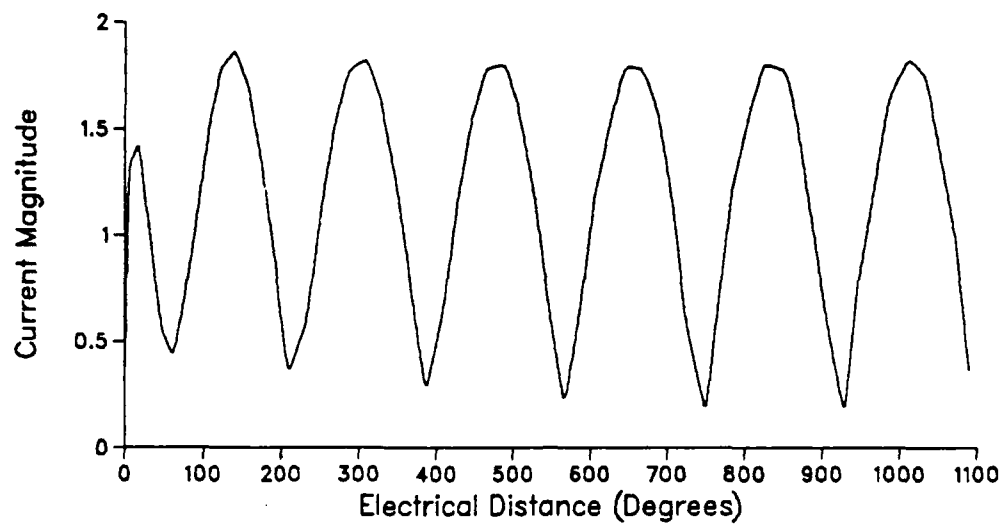


Figure 17. Current Distribution of Long Wire Antenna at 5 MHz.

564-FOOT LONGWIRE WITH SLANTED FEEDER / HEIGHT=40 FEET.  
OVER AVERAGE GROUND / ELEVATION PATTERN / FREQ=5 MHZ.

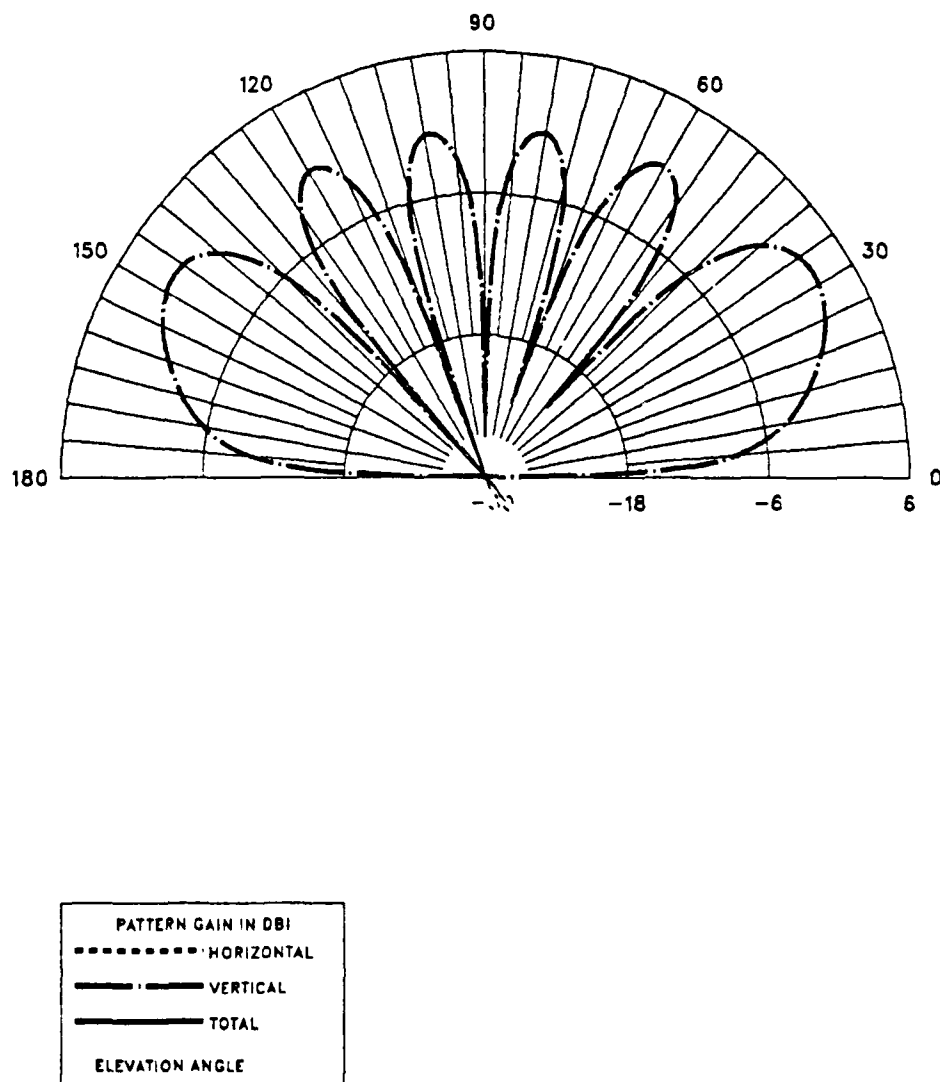


Figure 18. Elevation Pattern of Long Wire Antenna at 5 MHz.:  
 $\epsilon_r = 10.0, \sigma = 0.003$

564-FOOT LONGWIRE WITH SLANTED FEEDER / HEIGHT= 40 FEET.  
OVER AVERAGE GROUND / AZIMUTH PATTERN THETA=60 / FREQ=5 MHZ.

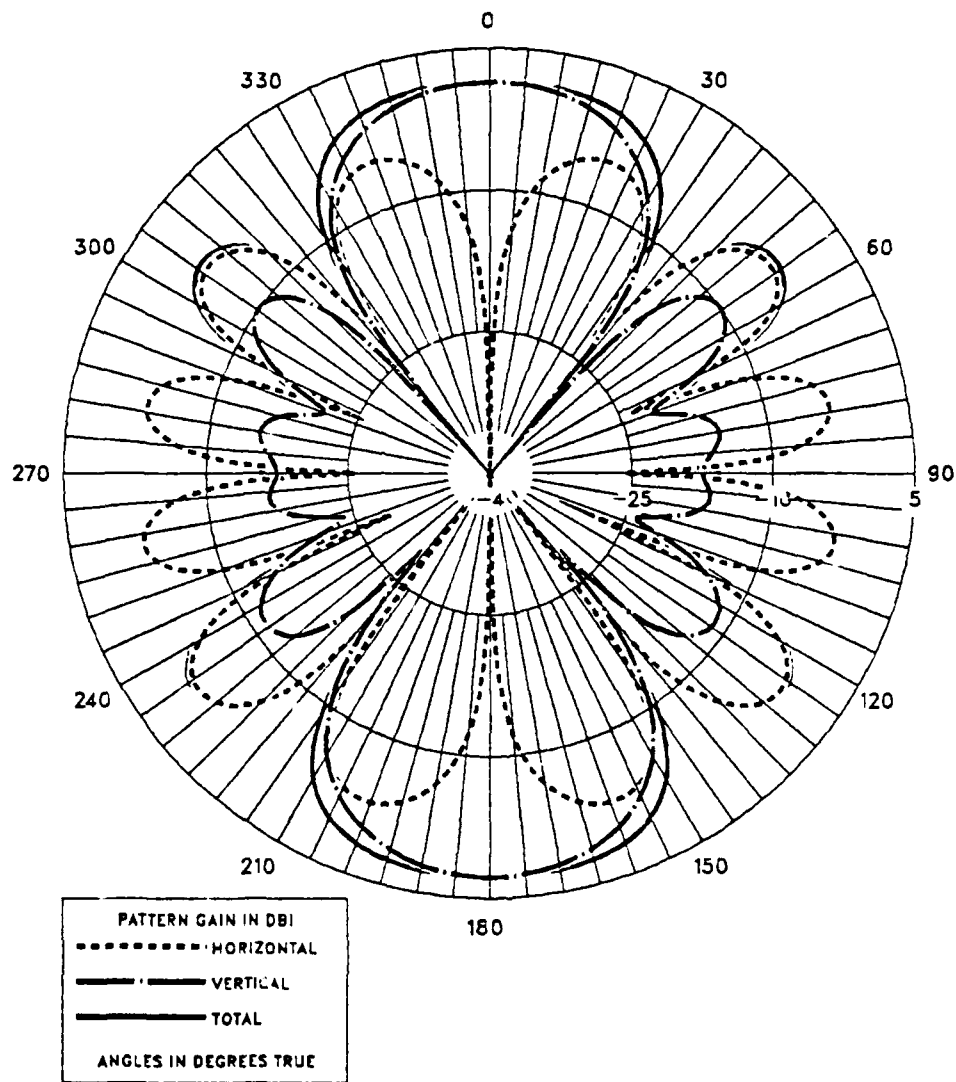


Figure 19. Azimuth Pattern of Long Wire Antenna at 5 MHz.  $\alpha = 30^\circ$ :  
 $\epsilon_r = 10.0$ ,  $\sigma = 0.003$



564-FOOT LONGWIRE WITH SLANTED FEEDER / HEIGHT= 40 FEET.  
OVER AVERAGE GROUND / AZIMUTH PATTERN THETA=30 / FREQ=5 MHZ.

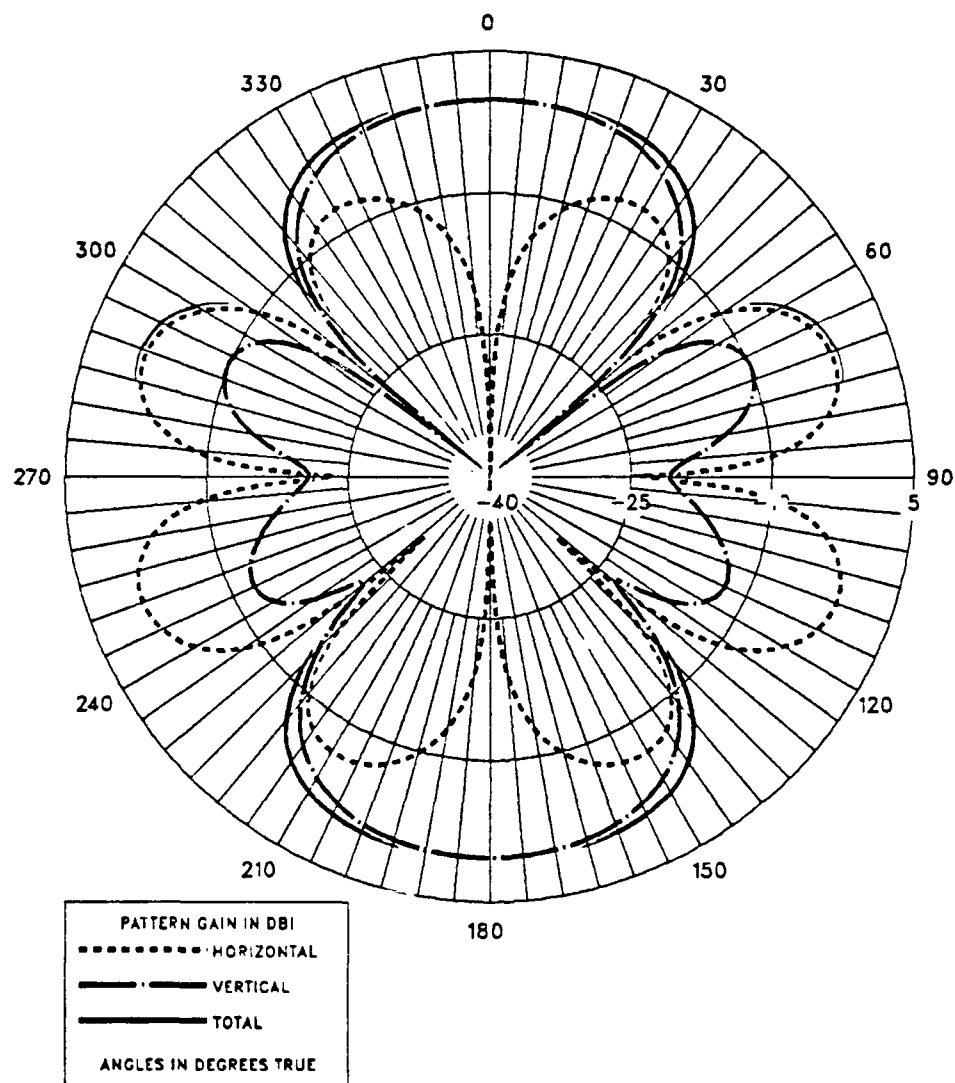


Figure 20. Azimuth Pattern of Long Wire Antenna at 5 MHz.  $\alpha = 60^\circ$ :  
 $\epsilon_r = 10.0, \sigma = 0.003$

564-FOOT LONGWIRE WITH SLANTED FEEDER / HEIGHT=40 FEET.  
OVER AVERAGE GROUND / AZIMUTH PATTERN THETA=10 / FREQ=5 MHZ.

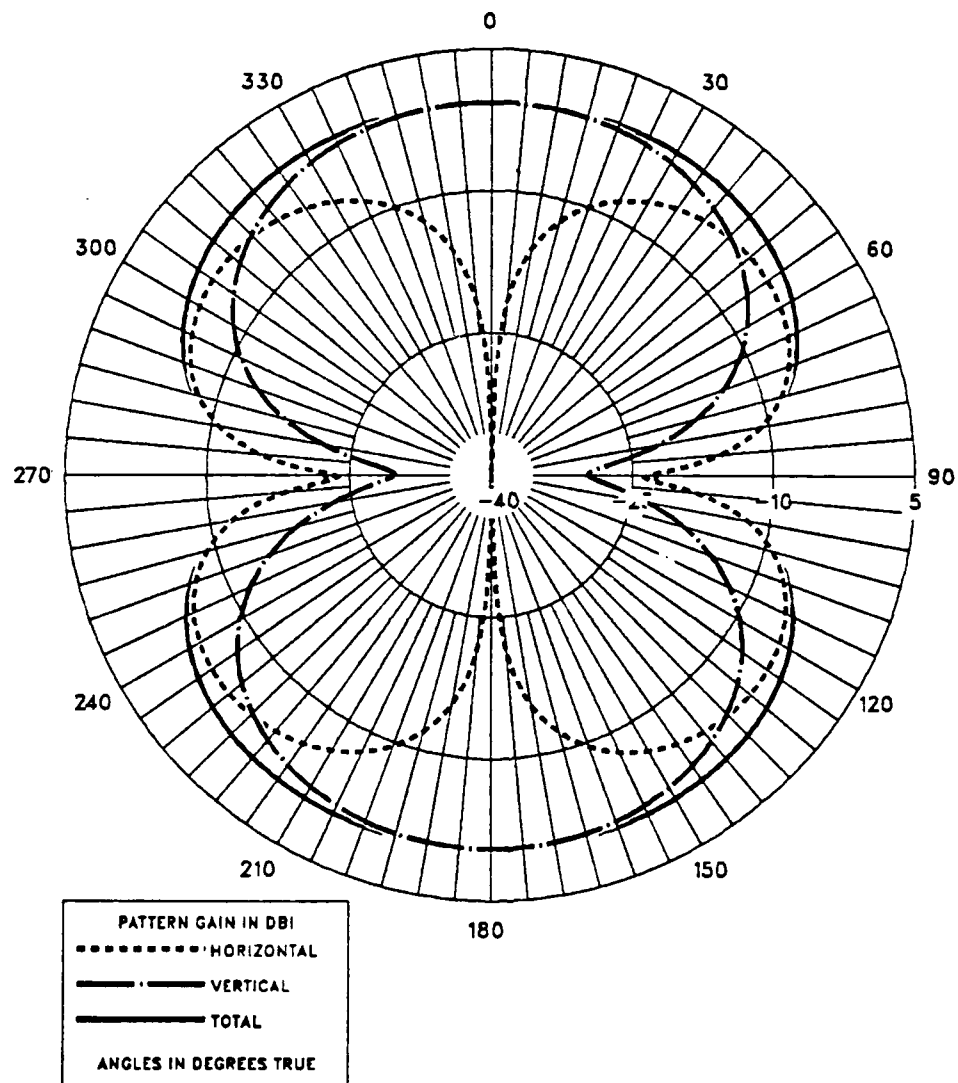


Figure 21. Azimuth Pattern of Long Wire Antenna at 5 MHz.  $\alpha = 80^\circ$ :  
 $\epsilon_r = 10.0$ ,  $\sigma = 0.003$

564-FOOT LONGWIRE WITH SLANTED FEEDER / FREQ= 30 MHZ.  
OVER AVERAGE GROUND / HEIGHT = 40 FEET.

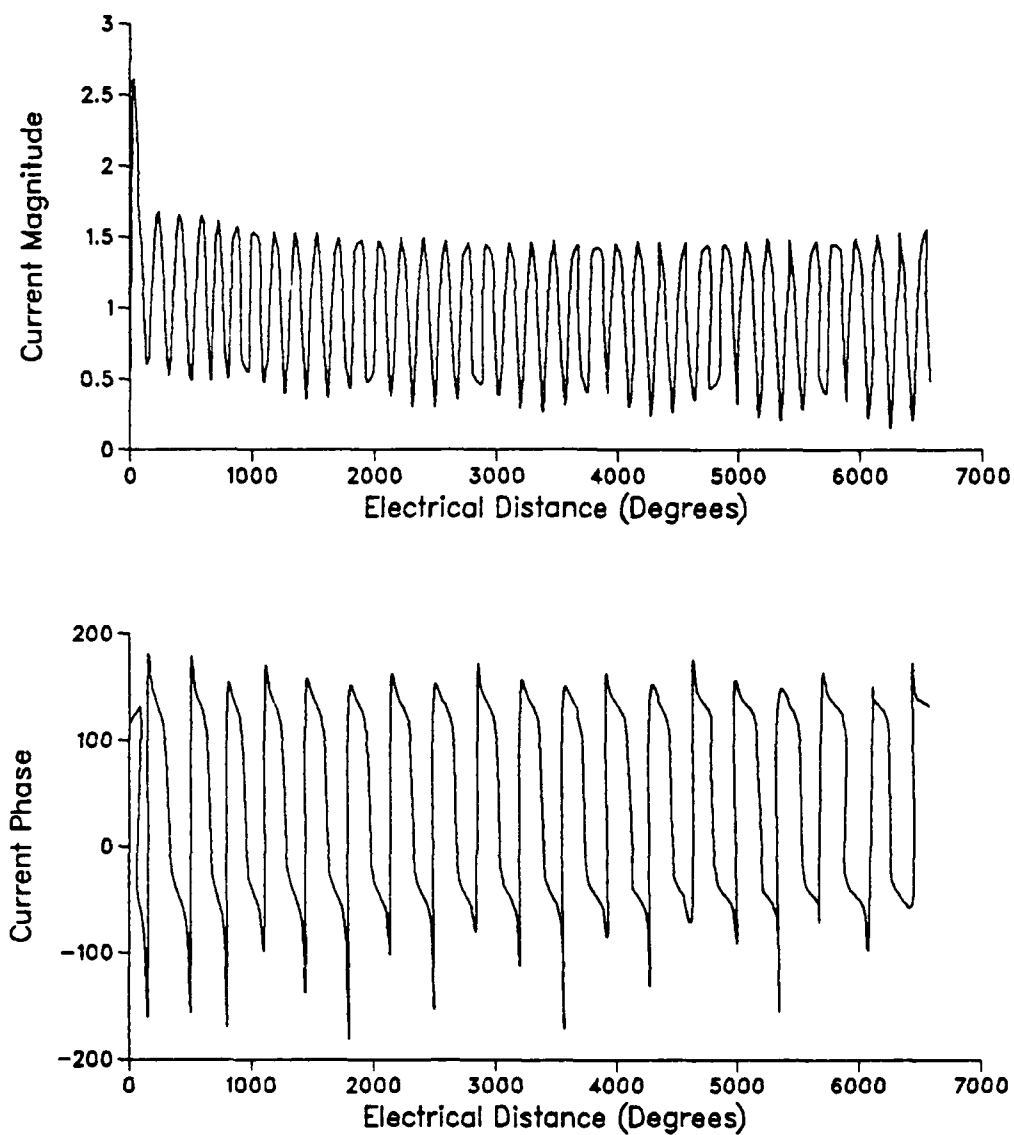


Figure 22. Current Distribution of Long Wire Antenna at 30 MHz.

564-FOOT LONGWIRE WITH SLANTED FEEDER / HEIGHT=40 FEET.  
OVER AVERAGE GROUND / ELEVATION PATTERN / FREQ=30 MHZ.

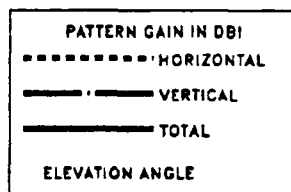
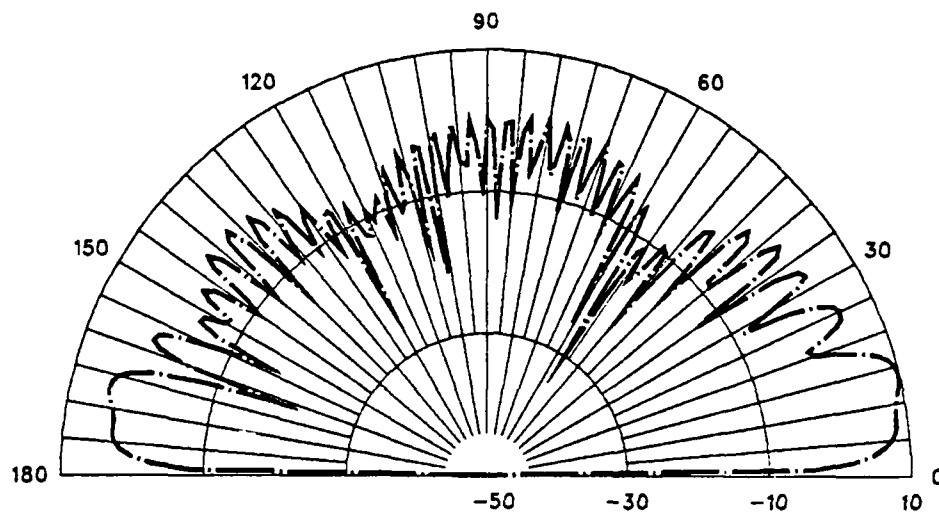


Figure 23. Elevation Pattern of Long Wire Antenna at 30 MHz.:

$$\epsilon_r = 10.0, \sigma = 0.003$$

564-FOOT LONGWIRE WITH SLANTED FEEDER / HEIGHT=40 FEET.  
OVER AVERAGE GROUND / AZIMUTH PATTERN THETA=75 / FREQ=30 MHZ

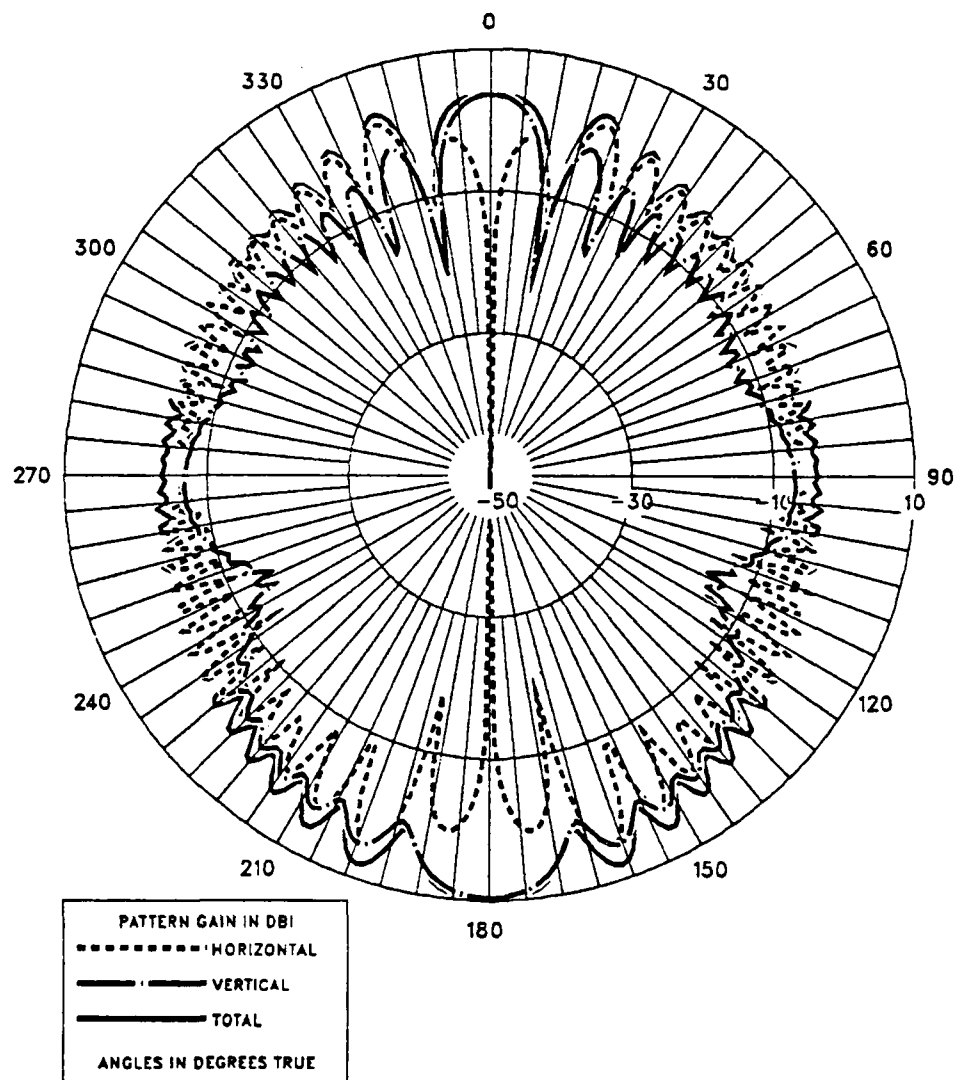


Figure 24. Azimuth Pattern of Long Wire Antenna at 30 MHz.  $\alpha = 15^\circ$ :  
 $\epsilon_r = 10.0, \sigma = 0.003$

564-FOOT LONGWIRE WITH SLANTED FEEDER / HEIGHT=40 FEET.  
OVER AVERAGE GROUND / AZIMUTH PATTERN THETA=65 / FREQ=30 MHZ

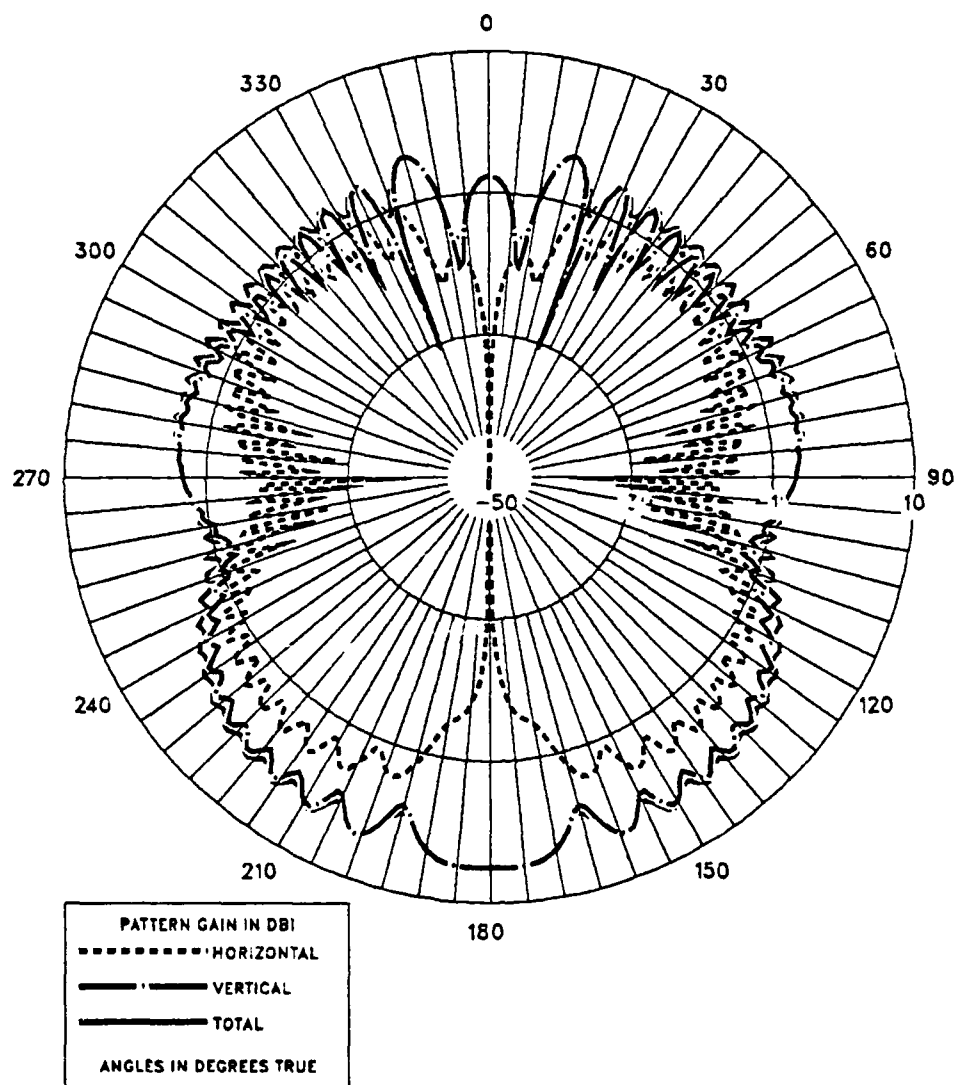


Figure 25. Azimuth Pattern of Long Wire Antenna at 30 MHz.  $\alpha = 25^\circ$ :  
 $\epsilon_r = 10.0, \sigma = 0.003$

### E. SLOPING VEE BEAM ANTENNA

This is a travelling-wave, balanced antenna. The angle between the descending wires was chosen so that the principal lobes of two radiators are superimposed. The mast height is chosen to make the antenna tilt angle the same as the take-off angle. Half of the radiated power is reflected from the ground. Therefore the ground should be smooth and free from obstructions. This antenna is horizontally polarized and has a relatively high input impedance.

The modeled antenna had two 528-foot descending wires. The interior angle between two wires was  $60^\circ$ . The feed point was 40 feet above the ground and each leg of the "Vee" was terminated through a  $600\ \Omega$  resistor to a 2 feet ground stake.

At 5 MHz each 528-foot leg has 45 segments. The load is placed on one segment at this frequency. The ground stake was modeled by 2 segments.

At 30 MHz each leg had 221 segments. The wire connecting the load to the ground stake has 4 tapered-length segments. Each ground stake was modeled with 4 segments. The gain at lower take-off angles provides good long range communication. Figure 33 shows the azimuth pattern at a  $10^\circ$  take-off angle. Although it is horizontally polarized, some of the radiated power comes from ground reflection.

For the current distribution on antenna wire No. 1,

$$I_1 = I_m e^{-jks} \quad (9)$$

and for the current distribution on antenna wire No. 2,

$$I_2 = I_m e^{-jks}$$

where  $I_m$  is the current amplitude and  $s$  is the distance from the feed point.

Figure 26 shows that the current distribution at 5 MHz is essentially a travelling wave sinusoidal current distribution. The magnitude decreases gradually toward the load and the phase reverses every half wavelength.

Figure 27 shows the elevation pattern of  $E_\theta$  at  $\phi = 60^\circ$ , the lobe created by one descending wire. Figure 28 shows the YZ-plane pattern plot of  $E_\theta$ . The lobe nearest to the antenna wire is the largest (the main lobe) and all others progressively diminish in strength. Figure 29 shows the azimuth plane pattern,  $E_\phi$ , at an elevation angle of  $20^\circ$ . The horizontal pattern gain in the direction of antenna is maximum and the back lobes are introduced by ground reflections. The input impedance is highly resistive. At this frequency the radiation resistance was calculated as

$$R_{rad} = \frac{1000}{|(1.1 + j0.006)(-1.1 - j0.006)|} = 762 \ \Omega. \quad (10)$$

Figure 30 demonstrates that the current distribution at 30 MHz is also a sinusoidal distribution with logarithmically decreasing magnitude.

At 30 MHz the antenna is about 16 wavelengths long. Figure 31 shows the elevation pattern at  $\phi = 60^\circ$ . Figure 32 shows also the YZ-plane pattern of  $E_\phi$ . Here the principles lobes are superimposed. The gain is maximum at a low take-off angle providing good long range communication. Figure 33 shows the azimuth pattern at a  $10^\circ$  take-off angle.

At this frequency radiation resistance was calculated as

$$R_{rad} = \frac{1000}{|(1.2 + j0.005)(-1.2 - j0.005)|} = 690 \ \Omega. \quad (11)$$



SLOPING "VEE BEAM" DIPOLE / ONE LEG / FREQ=5 MHZ.  
OVER AVERAGE GROUND / INCLUDING THE GND. STAKE CURRENT

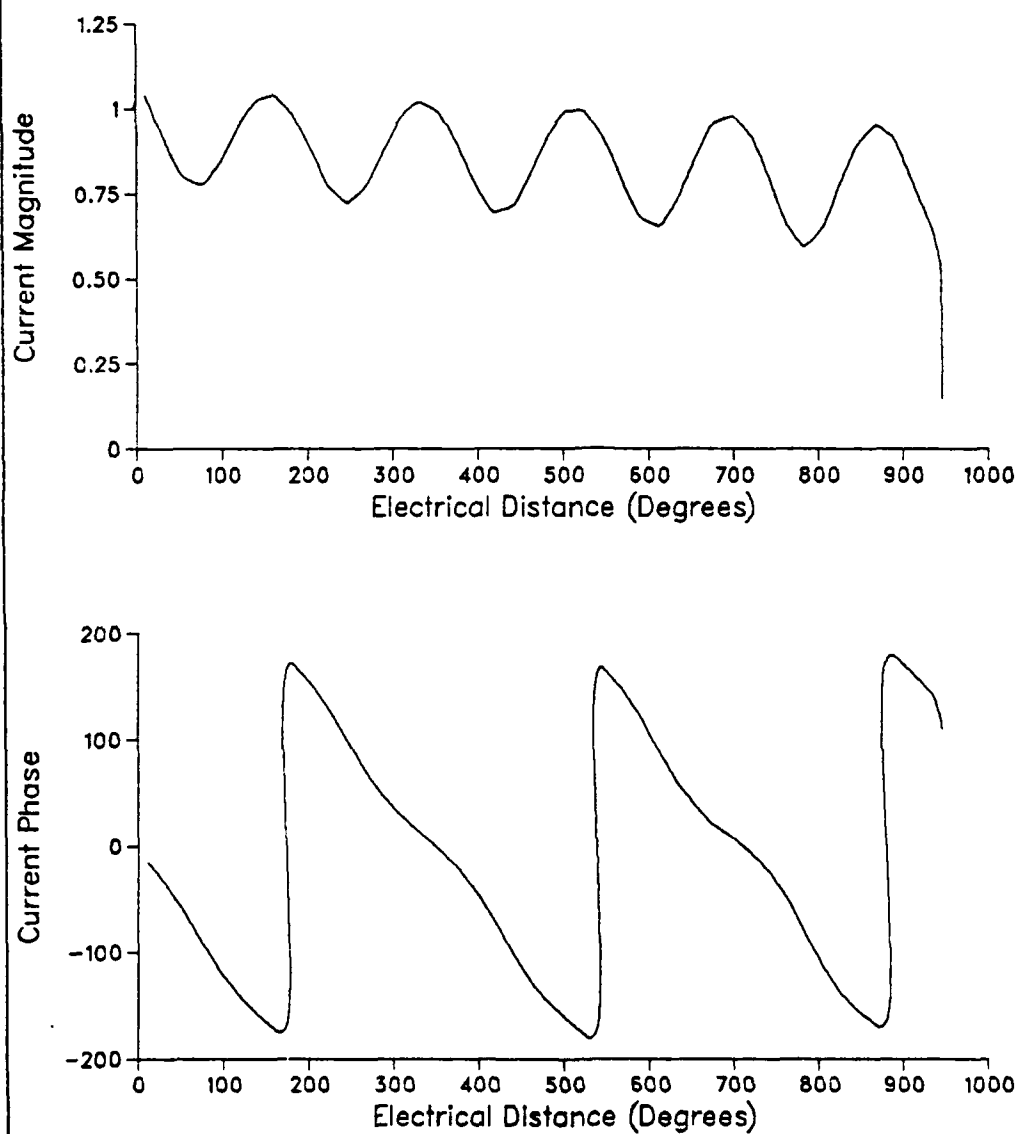


Figure 26. Current Distribution of Sloping Vee Antenna at 5 MHz.

SLOPING "VEE BEAM" DIPOLE / LENGTH OF EACH LEG = 528 FEET  
OVER AVERAGE GROUND / ELEVATION PATTERN  $\phi=60^\circ$  / FREQ=5 MHZ.

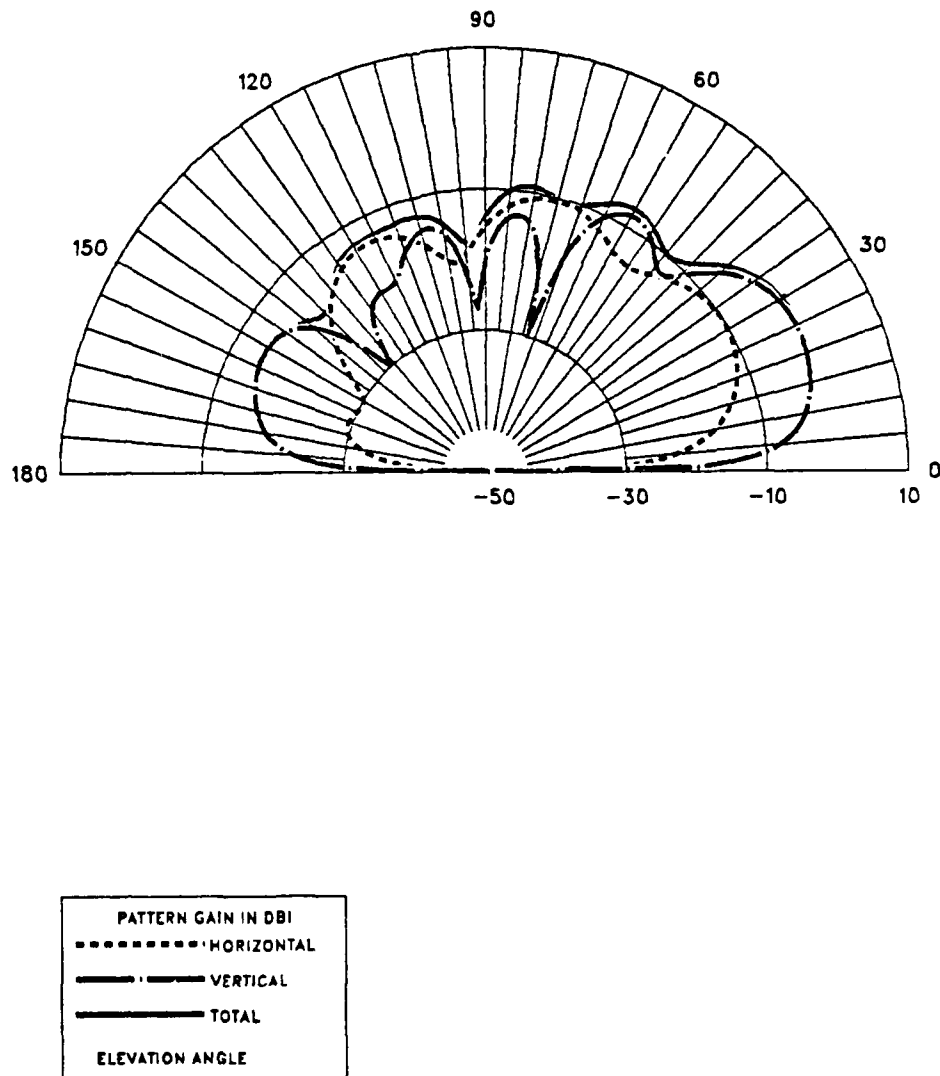


Figure 27. Elevation Pattern of Sloping Vee Antenna at 5 MHz.  $\phi = 60^\circ$ :  
 $\epsilon_r = 10.0, \sigma = 0.003$

SLOPING "VEE BEAM" DIPOLE / LENGTH OF EACH LEG = 528 FEET  
OVER AVERAGE GROUND / ELEVATION PATTERN PHI=90 / FREQ=5 MHZ.

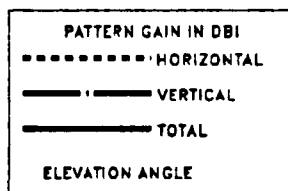
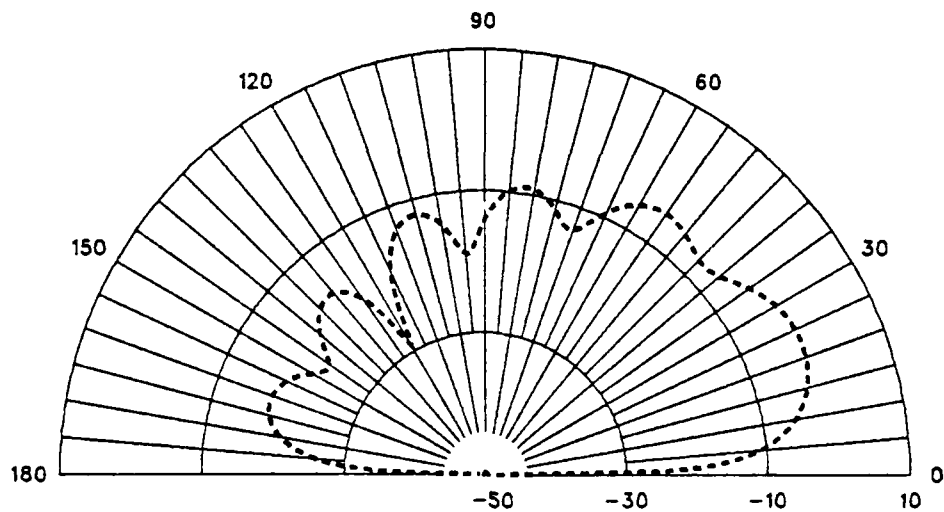


Figure 28. YZ-Plane Pattern of Sloping Vee Antenna at 5 MHz:

$\epsilon_r = 10.0, \sigma = 0.003$

SLOPING "VEE BEAM" DIPOLE / LENGTH OF EACH LEG = 528 FEET  
OVER AVERAGE GROUND / AZIMUTH PATTERN THETA=70 / FREQ=5 MHZ.

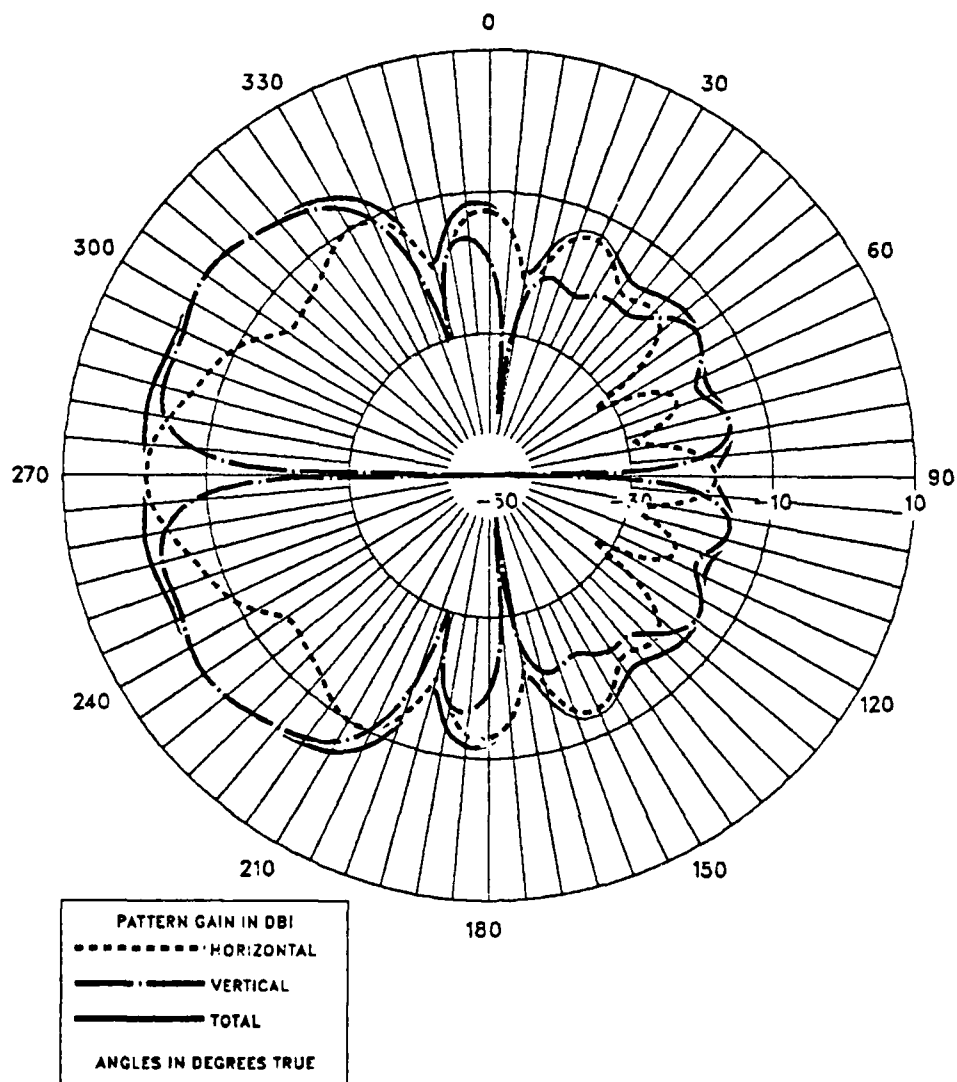


Figure 29. Azimuth Pattern of Sloping Vee Antenna at 5 MHz.  $\alpha = 20^\circ$ :  
 $\epsilon_r = 10.0$ ,  $\sigma = 0.003$

SLOPING "VEE BEAM" DIPOLE / ONE LEG / FREQ=30 MHZ.  
OVER AVERAGE GROUND / INCLUDING THE GND. STAKE CURRENT

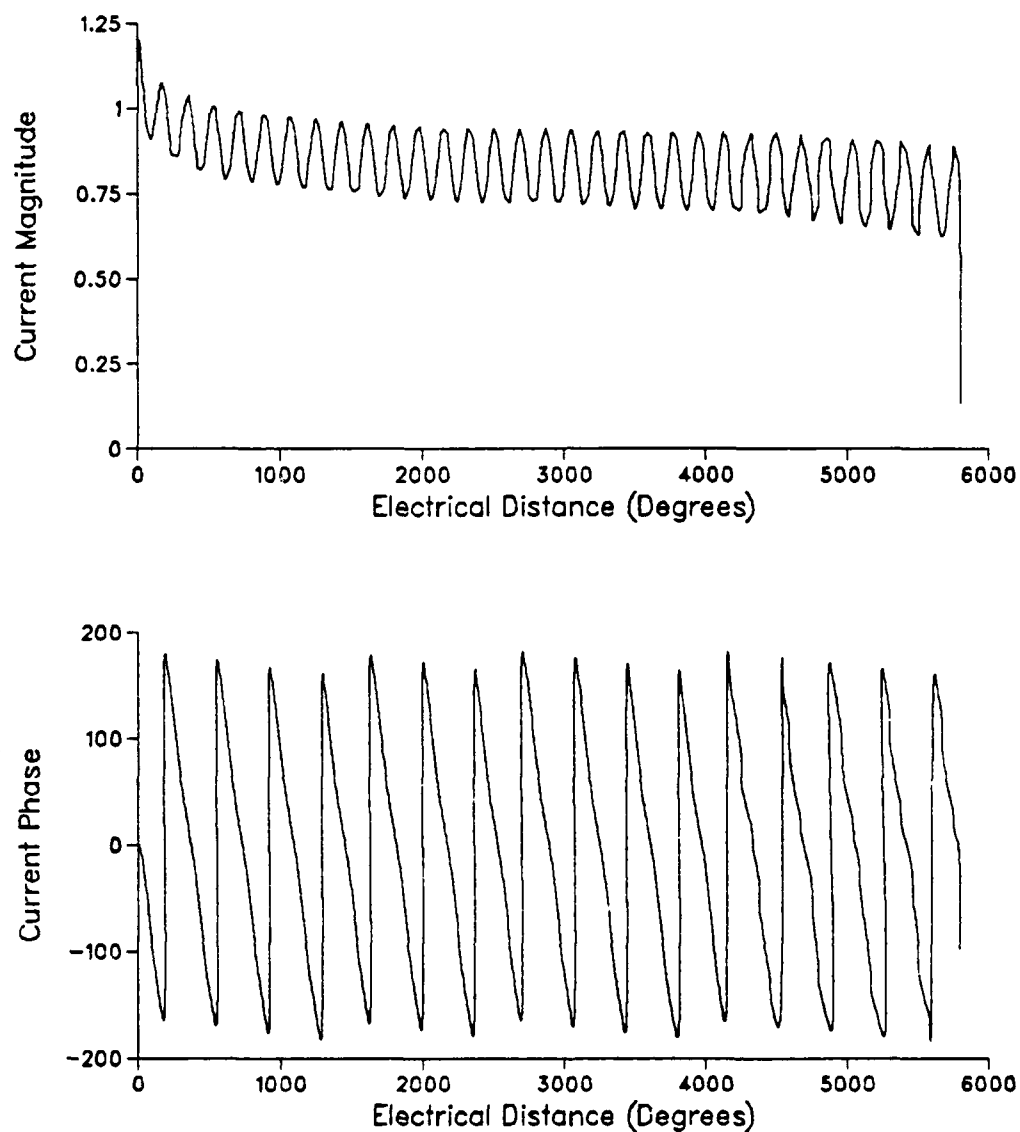


Figure 30. Current Distribution of Sloping Vee Antenna at 30 MHz.

SLOPING "VEE" BEAM DIPOLE / LENGTH OF EACH LEG = 528 FEET.  
OVER AVERAGE GROUND / ELEVATION PATTERN  $\phi=50$  / FREQ=30 MHZ

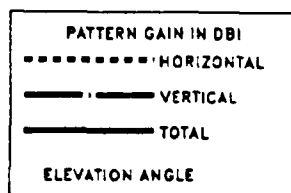
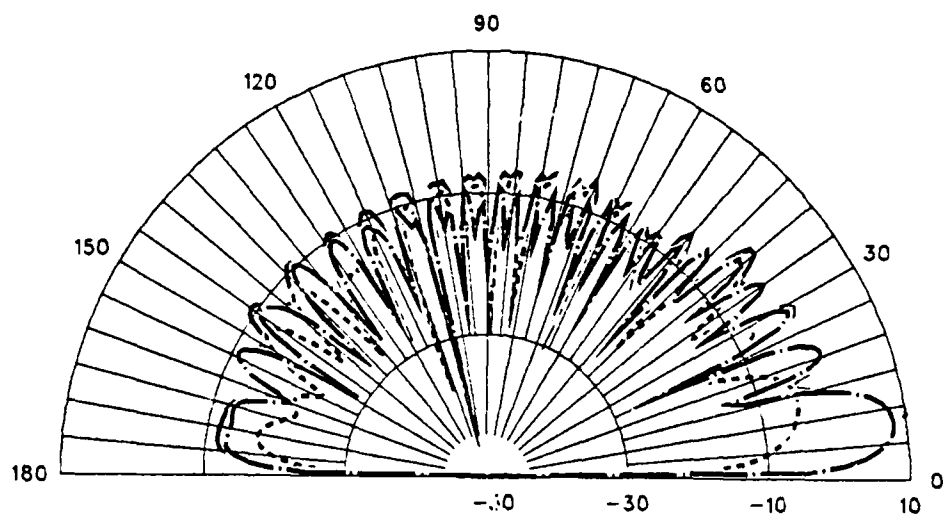


Figure 31. Elevation Pattern of Sloping Vee Antenna at 30 MHz.  $\phi = 60^\circ$ :  
 $\epsilon_r = 10.0$ ,  $\sigma = 0.003$

SLOPING "VEE" BEAM DIPOLE / LENGTH OF EACH LEG = 528 FEET.  
 OVER AVERAGE GROUND / ELEVATION PATTERN PHI=90 / FREQ=30 MHZ

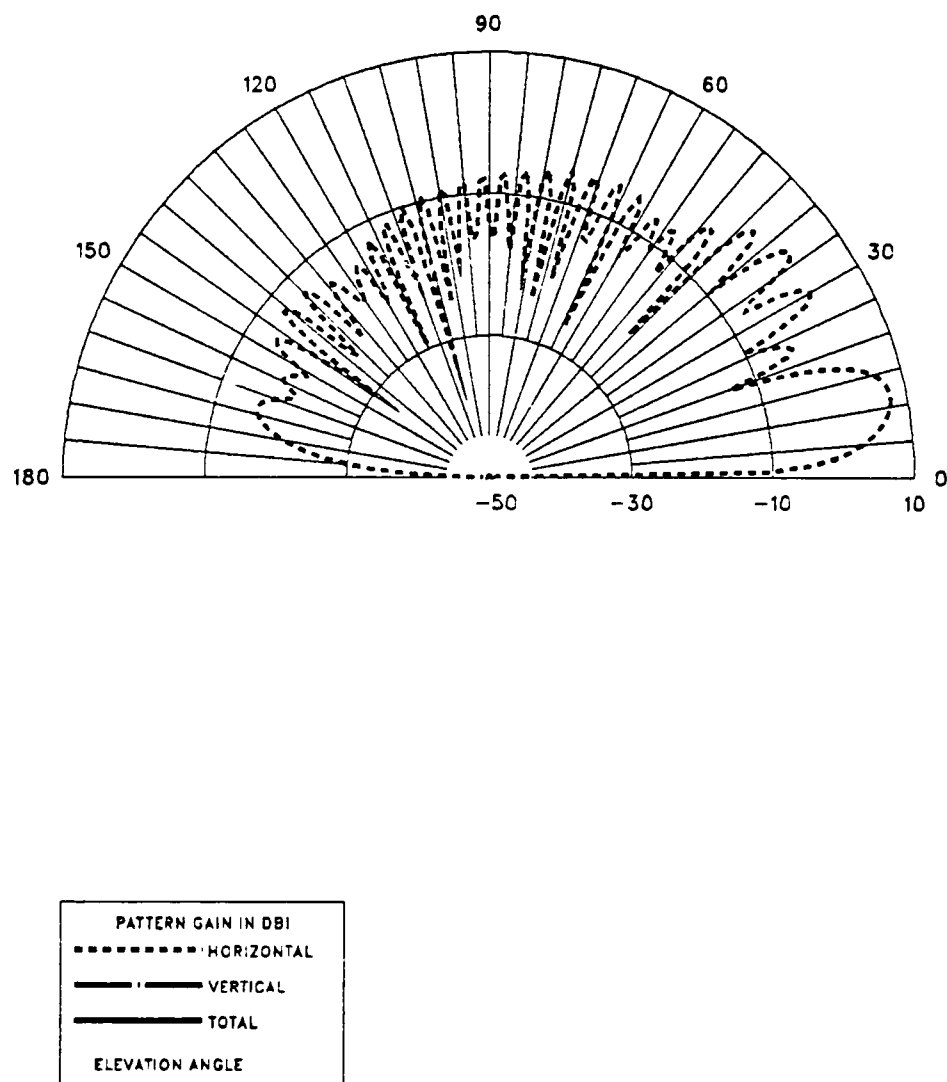


Figure 32. YZ-Plane Pattern of Sloping Vee Antenna at 30 MHz:  
 $\epsilon_r = 10.0, \sigma = 0.003$

SLOPING "VEE" BEAM DIPOLE / LENGTH OF EACH LEG  $\approx$  528 FEET.  
OVER AVERAGE GROUND / AZIMUTH PATTERN THETA=80 / FREQ=30 MHZ

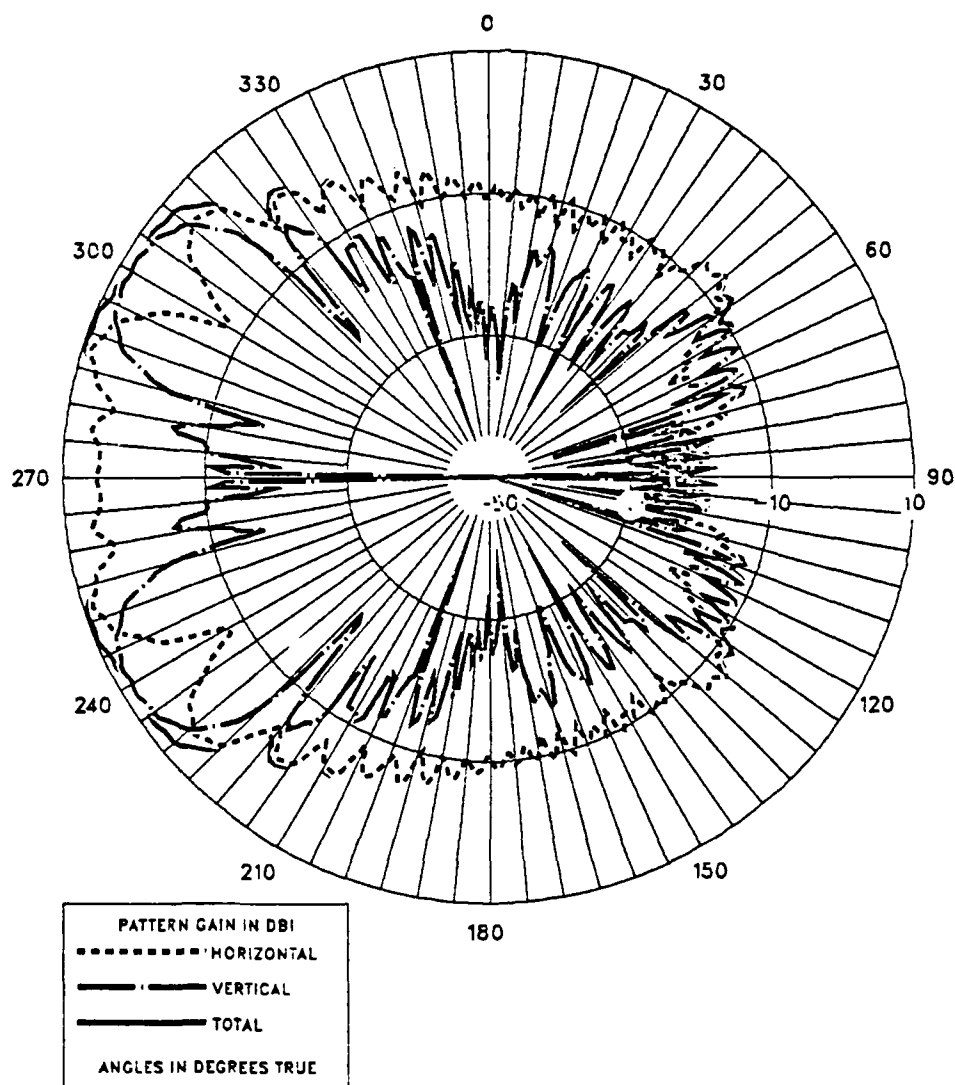


Figure 33. Azimuth Pattern of Sloping Vee Antenna at 30 MHz.  $\alpha = 10^\circ$ :  
 $\epsilon_r = 10.0$ ,  $\sigma = 0.003$



### III. CONCLUSIONS AND RECOMMENDATIONS

#### A. CONCLUSIONS

This thesis investigated the performance of 4 tactical HF field antennas at 5 and 30 MHz over average ground conditions.

The basic whip antenna provides good ground wave communication. The gain of the ground wave is proportional to the ground conductivity improvement. The skywave is not as dependant on ground constants. It has poor NVIS performance, but its low take-off angle favors long distance communication. At HF the usefulness of the basic whip is limited by the wide operating bandwidth usually required. The current distribution has the characteristics of standing waves.

The horizontal quad loop antenna has highest gain at high take-off angles. Therefore it has very poor ground wave performance. The radiation patterns show that it is good for NVIS and medium range skywave communications. The one wavelength quad loop has the same elevation and azimuth pattern as a half wavelength dipole, but it has more gain. Also the loop antenna has lower terminal resistance than a folded dipole. The current distribution is sinusoidal and continuous around the loop.

The long wire antenna allows short, medium, and long range communications. The radiation patterns at different frequencies show that as the frequency increases, the main lobe becomes more lobey and has better vertical gain at lower angles, providing long-range communication. The performance of the antenna remains practically unchanged within 10 MHz of the design center frequency. Generally, antennas which use terminated lines appear to have more radiation resistance than unterminated ones. Radiation and wire losses and the presence of ground and obstacles affect the pattern of any ideal source. If improvement is required, it is better to lengthen the longwire than to raise it. The height of the antenna can be adjusted so that the reflected wave combines in phase with the direct wave in the direction of maximum radiation. The important consideration here is the phase shift at the point of reflection [Ref. 11]. Since it is unterminated, a standing wave current distribution occurs along the antenna axis.

For the sloping "vee beam" antenna, it is also true that, like a longwire, this antenna has also a relatively wide bandwidth. Since half of the radiated power reflects from ground, the ground should be free from obstacles. The level of the sidelobes change considerably, depending on the type of ground. The level of the largest sidelobes is only

about 4 - 7 dB below the main beam. This is why the usefulness of the antenna is restricted. Its low take-off angle provides very good long-range communication. The current distribution is mainly that of travelling sinusoidal waves.

As a result, because of their well-known efficiency, the basic whip and quad loop can be used as reference standards for the spherical mode expansion work. The longwire and 528-foot sloping "vee beam " dipole are large, unwieldy and difficult to construct, but they are effective as base station antennas.

## **B. RECOMMENDATIONS**

The configurations of different antennas can be studied under different conditions or for different frequencies to provide more information for spherical modal expansion work, if needed.

## APPENDIX A. NEC AND AUXILIARY PROGRAMS

A brief description of some of the programs found in the NEC FORTRAN library are described below:

### 1. SOMNTX FOR SOMMERFELD / NORTON GROUND METHOD

This option can be requested on the GN card. This method is available for wires only. It uses an exact solution for the fields in the presence of ground and is accurate close to and beneath the ground. NEC reads interpolation tables from the file TAPE21. This input file must be created by running SOMNTX. SOMNTX reads 4 parameters from a data file:

- EPR = relative dielectric constant of ground (  $\epsilon_r$  )
- SIG = conductivity of ground in mho/m (  $\sigma$  )
- FMHZ = frequency in MHz.
- IPT = print option of interpolation tables.

### 2. THE NUMERICAL GREEN'S FUNCTION (NGF) OPTION

The main purpose of the NGF is to avoid unnecessary repetition of calculations. Another reason for using the NGF option is to exploit partial symmetry in a structure. This option can be requested by a WG card and a GF card.

### 3. DNPGNEC

A double precision version of NEC-2 available in mainframe at NPS, it is good for modeling structures up to 300 segments. DNPG1000, another version of NEC, is capable of handling up to 1000 segments.

### 4. PLOT PROGRAMS

- PLOTDGLP -- Plots data geometry to a laser printer.
- PLOTDG79 -- Plots data geometry to a 3279 terminal.
- PLOTTRPHM -- Plots horizontal and vertical components of radiation patterns. Use this to get azimuth plots in the horizontal plane.
- PLOTTRPVM -- Plots radiation pattern in the vertical plane.
- CURRPLOT -- This program plots current magnitude and phase for selected segments and tags or selected groups of segments or tags.

## **5. RVAL**

It is used for variable segmentation or tapered radius or both. RVAL asks the length of the first and the last segments and the total length of the wire. Then it calculates the segment lengths and the segmentation ratio. It is used on GC cards, which are read only when the radius on a GW card is set to zero.

## **6. DIRTLAM**

This program calculates the wavelength in dirt. The result is used to set segment lengths for wires buried under ground. It asks the relative dielectric constant, conductivity and operation frequency and gives the wavelength in the ground.

## APPENDIX B. NEC DATA SETS FOR CURRENTS

CM GEOMETRY : QUARTER WAVELENGTH BASIC WHIP WITH 8' GROUND ROD  
CM RADIO : NONE  
CM FREQUENCY : 5 MEGAHERTZ  
CM GROUND : EPSILON = 10; SIGMA = 0.003  
CE  
GW 1,6,0,0,0,0,0,14.989,0.015  
GW 2,3,0,0,0,0,0,-2.438,0.015  
GE 0,2  
FR 0,0,0,0, 5  
GN 2,0,0,0,10,.003  
EX 0,1,1,01,342.755  
PL 1,2,0,0  
XQ  
WG  
EN

CM GEOMETRY : QUARTER WAVELENGTH BASIC WHIP WITH 8' GROUND ROD  
CM RADIO : NONE  
CM FREQUENCY : 30 MEGAHERTZ  
CM GROUND : EPSILON = 10; SIGMA = .003  
CE  
GW 1,5, 0,0,0, 0,0,2.498, 0.015  
GW 2,15, 0,0,0, 0,0,-2.438, 0.015  
GE 0,2  
FR 0,0,0,0, 30,  
GN 2,0,0,0, 10,.003  
PL 1,2,0,0  
EX 0,1,1,01,336.641  
XQ  
WG  
EN

CM GEOMETRY : ONE WAVELENGTH HORIZONTAL QUAD LOOP  
CM HEIGHT = 0.25 WAVELENGTH  
CM CONDUCTOR = #12 AWG  
CM FREQUENCY : 5 MEGAHERTZ  
CM GROUND : EPSILON = 10; SIGMA = .003  
CE  
GW 1,12, 0,0,14.989, -10.599,10.599,14.989, 0.001  
GW 2,12, -10.599,10.599,14.989, 0,21.198,14.989, 0.001  
GW 3,12, 0,0,14.989, 10.599,10.599,14.989, 0.001  
GW 4,12, 10.599,10.599,14.989, 0,21.198,14.989, 0.001  
GE -1,2  
FR 0,0,0,0, 5,  
GN 2,0,0,0, 10,.003  
PL 1,2,0,0  
EX 0,1,1,01, 251.115  
EX 0,3,1,01, -251.115  
XQ

WG  
EN

CM GEOMETRY : ONE WAVELENGTH HORIZONTAL QUAD LOOP  
CM HEIGHT = 0.25 WAVELENGTH  
CM CONDUCTOR = #12 AWG  
CM FREQUENCY : 30 MEGAHERTZ  
CM GROUND : EPSILON = 10; SIGMA = .003  
CE  
GW 1,13, 0,0,2.498, -1.766,1.766,2.498, 0.001  
GW 2,13, -1.766,1.766,2.498, 0,3.532,2.498, 0.001  
GW 3,13, 0,0,2.498, 1.766,1.766,2.498, 0.001  
GW 4,13, 1.766,1.766,2.498, 0,3.532,2.498, 0.001  
GE -1,2  
FR 0,0,0,0, 30,  
GN 2,0,0,0, 10,.003  
PL 1,2,0,0  
EX 0,1,1,01, 252.345  
EX 0,3,1,01, -252.345  
XQ  
WG  
EN

CM GEOMETRY : 564-FOOT LONGWIRE WITH 45 DEGREE SLANTED FEEDER  
CM HEIGHT ABOVE GROUND = 40 FEET  
CM CONDUCTOR IS # 12 AWG  
CM FEEDER IS DRIVEN BY A VOLTAGE SOURCE WHOSE LOWER  
CM END IS TIED TO A 2-FOOT GROUND STAKE  
CM FREQUENCY : 5 MHZ  
CM GROUND : EPSILON = 10 ; SIGMA = .003  
CE  
GW 1,2, 0.0762,0.06096,-0.6096, 0.0762,0.06096,0  
GC 0,0, 1, 0.004,0.002  
GW 2,1, 0.0762,0.06096,0, 0.0762,0.06096,1.302, 0.001  
GW 3,8, 0.0762,0.06096,1.302, -10.8138,0.06096,12.192, 0.001  
GW 4,51, -10.8138,0.06096,12.192, -182.721,0.06096,12.192, 0.001  
GE -1,2  
FR 0,0,0,0, 5  
GN 2,0,0,0, 10,.003  
PL 1,2,0,0  
EX 0,3,1,01, 1204.350  
XQ  
WG  
EN

CM GEOMETRY : 564-FOOT LONGWIRE WITH 45 DEGREE SLANTED FEEDER  
CM HEIGHT ABOVE GROUND = 40 FEET  
CM CONDUCTOR IS # 12 AWG  
CM FEEDER IS DRIVEN BY A VOLTAGE SOURCE WHOSE LOWER  
CM END IS TIED TO A 2-FOOT GROUND STAKE  
CM FREQUENCY : 30 MHZ  
CM GROUND : EPSILON = 10 ; SIGMA = .003  
CE  
GW 1,4, 0.0762,0.06096,-0.6096, 0.0762,0.06096,0

GC 0,0, 1, 0.004,0.002  
 GW 2,6, 0.0762,0.06096,0, 0.0762,0.06096,1.302, 0.001  
 GW 3,45, 0.0762,0.06096,1.302, -10.8138,0.06096,12.192, 0.001  
 GW 4,200, -10.8138,0.06096,12.192, -182.721,0.06096,12.192, 0.001  
 GE -1,2  
 FR 0,0,0,0, 30  
 GN 2,0,0,0, 10,.003  
 PL 1,2,0,0  
 EX 0,3,1,01, 872.360  
 XQ  
 WG  
 EN

CM GEOMETRY : SLOPING "VEE BEAM" DIPOLE  
 CM APEX HEIGHT = 40 FEET  
 CM BOTH ENDS AT HEIGHT = 7 FEET  
 CM LENGTH OF EACH LEG OF "VEE" = 528 FEET  
 CM EACH LEG OF "VEE" IS TERMINATED THROUGH A 600-OHM  
 CM RESISTOR TO A 2-FOOT GROUND STAKE  
 CM INTERIOR ANGLE OF "VEE" = 60 DEGREES  
 CM CONDUCTOR IS # 12 AWG  
 CM FREQUENCY: 5 MHZ  
 CM GROUND : EPSILON = 10 ; SIGMA = .003  
 CE  
 GW 1,45, 0,0,12.192, 80.3099,139.1008,2.1336, 0.001  
 GW 2,1, 80.3099,139.1008,2.1336, 80.3099,139.1008,0, 0.001  
 GW 3,2, 80.3099,139.1008,0, 80.3099,139.1008,-0.6096  
 GC 0,0, 1, 0.002,0.004  
 GW 4,45, 0,0,12.192, -80.3099,139.1008,2.1336, 0.001  
 GW 5,1, -80.3099,139.1008,2.1336, -80.3099,139.1008,0, 0.001  
 GW 6,2, -80.3099,139.1008,0, -80.3099,139.1008,-0.6096  
 GC 0,0, 1, 0.002,0.004  
 GE -1,2  
 LD 4, 2,1,1, 600  
 LD 4, 5,1,1, 600  
 FR 0,0,0,0, 5  
 GN 2,0,0,0, 10,.003  
 PL 1,2,0,0  
 EX 0,1,1,01, 436.485  
 EX 0,4,1,01, -436.485  
 XQ  
 WG  
 EN

CM GEOMETRY : SLOPING "VEE BEAM" DIPOLE  
 CM APEX HEIGHT = 40 FEET  
 CM BOTH ENDS AT HEIGHT = 7 FEET  
 CM LENGTH OF EACH LEG OF "VEE" = 528 FEET  
 CM EACH LEG OF "VEE" IS TERMINATED THROUGH A 600-OHM  
 CM RESISTOR TO A 2-FOOT GROUND STAKE  
 CM INTERIOR ANGLE OF "VEE" = 60 DEGREES  
 CM CONDUCTOR IS # 12 AWG  
 CM FREQUENCY: 5 MHZ  
 CM GROUND : EPSILON = 10 ; SIGMA = .003  
 CE

GW 1,221, 0,0,12.192, 80.3099,139.1008,2.1336, 0.001  
GW 2,4, 80.3099,139.1008,2.1336, 80.3099,139.1008,0,  
GC 0,0,1.306,0.001,0.001  
GW 3,4, 80.3099,139.1008,0, 80.3099,139.1008,-0.6096  
GC 0,0, 1, 0.002,0.004  
GW 4,221, 0,0,12.192, -80.3099,139.1008,2.1336, 0.001  
GW 5,4, -80.3099,139.1008,2.1336, -80.3099,139.1008,0,  
GC 0,0,1.306,0.001,0.001  
GW 6,4, -80.3099,139.1008,0, -80.3099,139.1008,-0.6096  
GC 0,0, 1, 0.002,0.004  
GE -1,2  
LD 4, 2,4,4, 600  
LD 4, 5,4,4, 600  
FR 0,0,0,0, 30  
GN 2,0,0,0, 10,.003  
PL 1,2,0,0  
EX 0,1,1,01, 415.428  
EX 0,4,1,01, -415.428  
XQ  
WG  
EN



## APPENDIX C. NUMERICAL METHODS AND TECHNIQUES FOR ANTENNA ANALYSIS

### A. THE METHOD OF SOLUTION

NEC uses both an electric-field integral equation (EFIE) and a magnetic-field integral equation (MFIE). The EFIE in NEC is well-suited for thin-wire structures of small or vanishing conductor volume. MFIE is only useful for closed structures, especially those having large smooth surfaces. For a structure containing both wires and surfaces, the EFIE and MFIE are coupled in NEC.

To model wires, the thin wire approximation is used in the EFIE to reduce it to a scalar integral equation. The assumptions used are [Ref. 8] :

1. Transverse currents are neglected relative to axial currents on the wire.
2. The circumferential variation in the axial current is neglected.
3. The current is represented by a filament on the wire axis.
4. The boundary condition on the electric field is enforced in the axial direction only.

These approximations are valid for the wire radius much less than the wavelength and much less than the wire length. An alternative kernel for the EFIE, based on an extended thin-wire approximation, is also included in NEC for wires having too large a radius for the thin-wire approximation [Ref. 12]. With the thin-wire approximation the EFIE becomes:

$$-\hat{s} \cdot \bar{E}'(\bar{r}) = \frac{-j}{4\pi\omega\epsilon} \int_{c(\bar{r})} I(s') (\hat{s} \cdot \hat{s}' k^2 - \frac{\partial^2}{\partial s \partial s'}) g(\bar{r}, \bar{r}') ds' \quad (12)$$

where

- |                     |                                          |
|---------------------|------------------------------------------|
| $\hat{s}$           | = unit vector along the wire axis.       |
| $\hat{s}'$          | = distance along the wire axis.          |
| $\bar{E}'(\bar{r})$ | = incident electric field at $\bar{r}$ . |
| $\omega$            | = $2\pi f$ , where $f$ is frequency.     |
| $I(s')$             | = axial current.                         |
| $\epsilon$          | = permittivity.                          |

$$\begin{aligned}
k &= \omega\sqrt{\mu\epsilon} = \text{phase constant.} \\
\bar{r} &= \text{observation point.} \\
\bar{r}' &= \text{source point.} \\
g(\bar{r}, \bar{r}') &= \exp\left[\frac{-jkr}{R}\right] = \text{free space Green's function.} \\
R &= (\bar{r} - \bar{r}')
\end{aligned}$$

The MFIE for a closed surface  $S$  is:

$$\bar{J}_s(\bar{r}) = 2\hat{n} \times \bar{H}^{inc}(\bar{r}) + \frac{1}{2\pi} \hat{n} \times \int_S \bar{J}_s(\bar{r}') \times \nabla' g ds' \bar{r} \epsilon s' \quad (13)$$

where

$$\begin{aligned}
\bar{J}_s(\bar{r}) &= \text{surface current density.} \\
\bar{H}^{inc}(\bar{r}) &= \text{incident magnetic field at the observation point.} \\
\hat{n} &= \text{unit vector normal to the surface at } \bar{r}.
\end{aligned}$$

The integral equations (12) and (13) are solved numerically in NEC by a form of the method of moments. This solution includes expanding the unknown current in a summation of basis functions with unknown amplitudes and enforcing equality of weighted integrals of fields. The weighting functions for both wires and surfaces in NEC are chosen to be delta functions which resulted in a point sampling of the fields. Wires are divided into short segments with a sample point at the center of each segment. The surfaces are approximated by a set of flat patches or facets with a sample point at the center of each patch.

Delta functions are also used in NEC as the current expansion functions on a surfaces. For the MFIE, Galerkin's method [Ref. 13] provides good accuracy on large smooth surfaces. Due to nature of the integral-equation kernels, however, the choice of current expansion functions is more critical in the EFIE than the MFIE.

A more realistic representation of the surface current is needed where a wire connects to a surface than the delta function expansion normally used with the MFIE. In the region of the wire connection, the surface current includes a singular component due to the current flowing from the wire onto the surface.

As a result of the continuity conditions on current and charge there remains one unknown associated with each basis function to be determined by solving the electromagnetic interaction equations. Enforcing appropriate conditions on the current

and charge results in rapid convergence of the solution. The conditions may be inappropriate in some cases, such as for short segments at a change in radius and at junctions of closely spaced wires. The result is then slower convergence. More accurate conditions for these cases are currently being developed for NEC [Ref. 8].

## **B. CAPABILITIES OF NEC**

There are basically two versions of NEC written in FORTRAN. NEC-2 has no distribution restrictions and limited a maximum of 300 segments to model a given structure. On the other hand NEC-3 is classified as Defense Critical Technology and can be released only to DoD agencies and their contractors without specific DoD approval. NEC-3 can be used up to 300, 1000, or 2000 segments, depending on the versions of NEC being used. The capabilities of these codes are summarized below.

### **1. Input**

A user-oriented data card set for a single run consists of three types of data cards. The deck must begin with one or more comment cards which can contain a brief description and structure parameters for the run. These are followed by geometry data cards which permits defining straight wires, arcs, and surfaces. Electrical connections are determined in the program by searching for wire ends and patch centers that coincide. Shifts, rotation, and reflections can be used in building structures. Finally, a section of program control cards specifies electrical parameters such as frequency, loading and excitation, and requests calculation of antenna currents and fields.

### **2. Output**

Outputs are selectable by input parameters and may include one or more following data:

1. charge density on wires.
2. current.
3. input impedance, admittance, and power.
4. radiated power, ohmic loss, efficiency.
5. radiated field, power gain and directive gain.
6. average gain.
7. near E and H fields.
8. maximum coupling.
9. receiving patterns.
10. scattering cross sections.

### **3. Source modeling**

A structure may be excited by one of the following sources:

1. voltage source (applied-E-field source).
2. incident plane wave, linear polarization.
3. incident plane wave, right-hand elliptic polarization.
4. incident plane wave, left-hand elliptic polarization.
5. elementary current source.
6. voltage source (current-slope-discontinuity).

### **4. Nonradiating Networks and Transmission lines**

Nonradiating two-port networks and transmission lines may connect points on wires. The defining parameters are characteristic impedance, length, and shunt admittance.

### **5. Loading**

Lumped or distributed RLC loads may be specified on wires. The options that the user can specify are:

1. series RLC, input ohms, henries, farads.
2. parallel RLC, input ohms, henries, farads.
3. series RLC, input ohms meter, henries meter, farads/meter.
4. parallel RLC, input ohms meter, henries meter, farads meter.

Also the conductivity of a round wire may be specified and the impedance computed taking account of skin depth.

### **6. Ground Effects**

For an antenna structure in or near the ground, there are three options available. A perfectly conducting ground is modeled by including the image field in the kernel of the integral equations. An approximate model for a finitely conducting ground uses the image modified by Fresnel reflection coefficients. This approximation is usable for antennas at least 0.1 to 0.2 wavelengths above the ground.

NEC-3 includes an accurate treatment for wire structures above, below, or penetrating the ground surface. The solution is based on the Sommerfeld integral formulation for the field near the interface.

## 7. Modeling Guidelines

Some of the guidelines for modeling are summarized below.

For accurate results, the lengths of wire segments should be less than about  $0.1 \lambda$ . Longer segments up to about  $0.14 \lambda$  may be acceptable on long straight wires or noncritical parts of a structure. For critical regions, shorter segments  $0.05 \lambda$  or less may be needed. The minimum segment length set by the computational precision is about  $10^{-4} \lambda$ . In double precision the minimum length is about  $10^{-8} \lambda$ .

The wire radius,  $a$ , relative to  $\lambda$  is limited by approximations used in the kernel of the EFIE. Two options are available, the thin-wire kernel and the extended thin-wire kernel. With the extended thin-wire kernel the ratio of segment length to radius can be as small as 0.5. With the thin-wire approximation, the limit is 2. In either case, only currents in the axial direction on a segment are considered, and there is no allowance for variation of the current around the wire circumference. The acceptability of these approximations depends on both the value of  $a/\lambda$  and the tendency of the excitation to produce circumferential currents. Discontinuities in wire radius should be kept to less than a factor of two.

Electrically small loops present special accuracy problems. In single precision the minimum loop circumference is about  $0.002 \lambda$ ; while in double precision it is about  $10^{-4} \lambda$ .

The surfaces modeled with patches must be closed. A reasonable maximum for the area of a surface patch appears to be 0.04 square wavelengths.

An important consideration in using NEC is the solution time versus model size since this may limit the amount of detail that can be modeled and the segment and patch densities. For a model using  $N$  wire segments, the solution time in seconds on a CDC computer is approximately [Ref. 8]

$$T = 3(10^{-4})kN^2/M + 2(10^{-6})N^3/M^2 \quad (14)$$

where  $M$  is the number of degrees of symmetry and  $k$  is 1 for free space, 2 for perfectly conducting ground modeled with the reflection coefficient approximation, and 4 to 8 for Sommerfield integral treatment of finitely conducting ground.

The first term in Eq. (3) is the time to fill the interaction matrix and the second term is the time to factor it into triangular parts for solution. For a model using  $N_p$  patches, the solution time is about [Ref. 8]

$$T = (10^{-5})k(2N_p)^2/M + 2(10^{-6})(2N_p)^3/M^2 \quad (15)$$

since two rows and columns in the matrix are associated with each patch.

When the Sommerfeld ground treatment is used, a fixed time of about 15 seconds [Ref. 8] is needed to generate the interpolation tables. The tables depend only on the ground parameters and frequency, and can be saved for use in any case in which these parameters are the same.

### C. CONCLUSION

NEC is a versatile code for modeling antennas and their environment including transmission lines, networks, loading and ground effects. It is written in FORTRAN and consists of about 10,000 lines of code.

Recently released extensions of NEC include a model for insulated wires and improved accuracy in modeling electrically small antennas and discontinuities in wire radius. A long-range goal is to incorporate expert-systems technology to simplify the process of building models that conform to the modeling guidelines and to verify that the code is producing correct results [Ref. 8].

NEC will continue to be a widely used antenna modeling program, due to its convenient operation, documentation, availability, and continuing support.

## LIST OF REFERENCES

1. Breakall, J. K., Domning, E. E., Christman, A. M., Averill, W. P., and Hayden, J. S., *Antenna Engineering Handbook, Vols. 1 to 7*, LLNL Tech. Report, UCRL--21031, Nov. 1987.
2. Burke, G. J., and Poggio, A. J., *Numerical Electromagnetics Code (NEC)-Method of Moments*, LLNL Tech. Report, UCID--18834, Jan. 1980.
3. Averill, W. P., *Appendix C, Sorted Antenna Performance Tables, Fair Ground*, pp. 1-23, Unpublished material, 1988.
4. Harrington, R. F., *Time Harmonic Electromagnetic Fields*, McGraw-Hill, 1961, Chapter 6, Spherical Wave Functions.
5. Schelkunoff, S. A., *Advanced Antenna Theory*, John Wiley and Sons, 1952, Chapter 2, Mode Theory of Antennas.
6. Schelkunoff S. A., and Friis H. T., *Antennas: Theory and Practice*, John Wiley and Sons, 1952, Chapter 4, Spherical Waves.
7. Breakall, J. K., *Research Proposal for PC Antenna Engineering Handbook*, 1 May 1989 -- 30 September 1989, submitted to US Army Information Systems, Ft. Huachuca, Arizona. (Unpublished material).
8. Burke, G. J., *Present Capabilities and New Developments in Antenna Modeling with the Numerical Electromagnetics Code NEC*, Lawrence Livermore National Laboratory, UCRL-98107, April 1988.
9. Strauch, J., and Thompson S., *Interactive Graphics Utility for Army NEC Automation (IGUANA)*, Naval Ocean Systems Center, Rept. CR 308, 1985.

10. Li, S. T., Logan, J. C., Rockway, J. W., and Tam D. W., *Microcomputer Tools for Communication Engineering*, Artech House, Inc., Dedham MA, 1983.
11. Ma, M., *Theory and Application of Antenna Arrays*, John Wiley and Sons, 1974, Chapter 6, Travelling-wave antennas above lossy ground.
12. Poggio, A. J., and Adams R. W., *Approximations for Terms Related to the Kernel in Thin-wire Integral Equations*, Lawrence Livermore National Laboratory, Rept. UCRL-51985, 1975.
13. Stutzman W. L., and Thiele G. A., *Antenna Theory and Design*, John Wiley and Sons, 1981, Chapter 7, Moment Methods.



## INITIAL DISTRIBUTION LIST

		No. Copies
1.	Defense Technical Information Center Cameron Station Alexandria, VA 22304-6145	2
2.	Library, Code 0142 Naval Postgraduate School Monterey, CA 93943-5002	2
2.	Chairman, Code EC Department of Electrical and Computer Engineering Naval Postgraduate School Monterey, CA 93943-5000	1
3.	Director, Research Administration, Code 012 Naval Postgraduate School Monterey, CA 93943-5000	1
4.	Naval Postgraduate School Dr. Richard W. Adler, Code EC/Ab Monterey, CA 93943-5000	5
5.	Naval Postgraduate School Prof. S. Jauregui, Code EC/Ja Monterey, CA 93943-5000	1
6.	Penn State University ATTN: J. K. Breakall, CSSL 211 EE East University Park, PA 16802	5
7.	University of S. Carolina ATTN: Dr. T. L. Simpson College of Engineering Columbia, SC 29208	2
8.	U.S. Army Information Systems Engineering and Integration Center ATTN: Commander (Janet McDonald, ASB-SET-P) Ft. Huachuca, AZ 85613-5300	5
9.	Gnkur. Bsk. ligi Muhabere Bilgi Destek Daire Bsk. ligi Bakanliklar - ANKARA - TURKEY	1
10.	Kara Kuvvetleri Komutanligi Muhabere Bsk. ligi Bakanliklar - ANKARA - TURKEY	1